

A Critical Evaluation of Proxy Methods used to Estimate the Acidity of Atmospheric Particles

C. J. Hennigan¹, J. Izumi¹, A. P. Sullivan², R. J. Weber³, and A. Nenes^{3,4,5}

[1] Department of Chemical, Biochemical and Environmental Engineering, University of Maryland, Baltimore County

[2] Department of Atmospheric Science, Colorado State University

[3] School of Earth and Atmospheric Sciences, Georgia Institute of Technology

[4] School of Chemical and Biomolecular Engineering, Georgia Institute of Technology

[5] Foundation for Research and Technology – Hellas, Patras, Greece

Correspondence to: C. J. Hennigan (hennigan@umbc.edu)

Abstract

Given significant challenges with available measurements of aerosol acidity, proxy methods are frequently used to estimate the acidity of atmospheric particles. In this study, four of the most common aerosol acidity proxies are evaluated and compared: 1) the ion balance method, 2) the molar ratio method, 3) thermodynamic equilibrium models, and 4) the phase partitioning of ammonia. All methods are evaluated against predictions of thermodynamic models and against direct observations of aerosol-gas equilibrium partitioning acquired in Mexico City during the MILAGRO study. The ion balance and molar ratio methods assume that any deficit in inorganic cations relative to anions is due to the presence of H^+ ; and that a higher H^+ loading and lower cation/anion ratio both correspond to increasingly acidic particles (i.e., lower pH). Based on the MILAGRO measurements, no correlation is observed between H^+ levels inferred with the ion

1 balance and aerosol pH predicted by the thermodynamic models and $\text{NH}_3\text{-NH}_4^+$ partitioning.
2 Similarly, no relationship is observed between the cation/anion molar ratio and predicted aerosol
3 pH. Using only measured aerosol chemical composition as inputs without any constraint for the
4 gas phase, the E-AIM and ISORROPIA-II thermodynamic equilibrium models tend to predict
5 aerosol pH levels that are inconsistent with the observed $\text{NH}_3\text{-NH}_4^+$ partitioning. The modeled
6 pH values from both E-AIM and ISORROPIA-II run with gas + aerosol inputs agreed well with
7 the aerosol pH predicted by the phase partitioning of ammonia. It appears that 1)
8 thermodynamic models constrained by gas + aerosol measurements, and 2) the phase partitioning
9 of ammonia provide the best available predictions of aerosol pH. Furthermore, neither the ion
10 balance nor the molar ratio can be used as surrogates for aerosol pH, and published studies to
11 date with conclusions based on such acidity proxies may need to be reevaluated. Given the
12 significance of acidity for chemical processes in the atmosphere, the implications of this study
13 are important and far reaching.

14
15
16
17

1 **1 Introduction**

2 The acidity of atmospheric particles is a critical parameter that affects air quality and the health
3 of aquatic and terrestrial ecosystems. Acute and chronic exposures to acidic particles have been
4 linked to deleterious effects in people, although the underlying physiological mechanisms are
5 unclear (Gwynn et al., 2000; Dockery et al., 1996). The deposition of acidic gases and particles
6 has been known for decades to damage freshwater and terrestrial ecosystems (Schindler, 1988;
7 Johnson et al., 2008). While the trends in emissions are promising in the U.S. and western
8 Europe, ecosystem recovery from the effects of acid deposition is a slow process that can take
9 decades (Likens et al., 1996; Stoddard et al., 1999). This may be a source of emerging
10 environmental crisis in places such as China, where acid deposition is increasing due to rapid
11 industrialization (Pan et al., 2013; Cao et al., 2013). Particle acidity also affects global
12 biogeochemical cycles by controlling the solubility – and thus, bioavailability – of limiting
13 nutrients that are delivered through atmospheric deposition in many marine environments
14 (Meskhidze et al., 2005; 2003; Nenes et al., 2011). This has important implications for marine
15 primary productivity, the carbon cycle, and even climate (Mahowald, 2011).

16 Particle acidity is also a critical factor that influences many chemical processes in the
17 atmosphere. The oxidation of S(IV) to S(VI) in liquid water, the primary pathway of sulfate
18 formation, is highly sensitive to pH (Chameides, 1984). Halogen chemistry is strongly
19 influenced by particle acidity, which has direct implications for the oxidation of volatile organic
20 compounds (VOCs) and ozone formation in marine and coastal regions (e.g., Keene et al., 1998;
21 Sander and Crutzen, 1996; Pszenny et al., 2004). Recent evidence has demonstrated that aerosol
22 pH is also a critical parameter influencing halogen chemistry in continental locations (Brown et
23 al., 2013; Thornton et al., 2010; Young et al., 2013). Further, aerosol acidity directly affects the

1 deposition and lifetime of many compounds in the atmosphere through its influence on the gas-
2 particle partitioning of semi-volatile species, including ammonia (NH_3), nitric acid (HNO_3), and
3 organic acids (Ahrens et al., 2012; Keene et al., 2004). Aerosol acidity may affect secondary
4 organic aerosol (SOA) formation, as well (e.g., Gaston et al., 2014; Surratt et al., 2007), although
5 the atmospheric importance of this phenomenon remains highly uncertain (Peltier et al., 2007;
6 Takahama et al., 2006; Tanner et al., 2009; Zhang et al., 2007; Xu et al., 2015).

7 Despite its significance, aerosol acidity remains very poorly constrained in the
8 atmosphere (Keene et al., 1998). All direct measurements employ filter sampling (e.g., Jang et
9 al., 2008; Keene et al., 2002; Koutrakis et al., 1988), which is both labor intensive and limited by
10 poor time resolution. Measurements are also challenged by the non-conservative nature of H^+ :
11 due to buffering effects and the partial dissociation of weak acids, H^+ concentrations do not scale
12 in proportion to the level of dilution (e.g., in aqueous filter extracts). Certain methods are also
13 susceptible to sampling artifacts, which can greatly increase the uncertainty of an inherently
14 challenging measurement (Pathak et al., 2004). Due to these limitations, indirect methods are
15 frequently employed to estimate the acidity of atmospheric particles. These methods include 1)
16 the ion balance method, 2) the molar ratio, 3) thermodynamic equilibrium models, and 4) the
17 phase-partitioning of semi-volatile species (HCl , NH_3 , HNO_3). The purpose of this study is to
18 evaluate and compare the proxy methods most commonly used to estimate aerosol acidity.

19 **2 Methods to Infer pH**

20 Before proceeding with this analysis, it is necessary to define the different physical
21 quantities commonly described by the term ‘aerosol acidity’. First, it is used to represent the pH
22 of an aerosol particle or distribution. The pH represents the hydrogen ion activity in an aqueous
23 solution (Stumm and Morgan, 1996):

1 $\text{pH} = -\log(\gamma^*x_{H^+})$ (1)

2 where γ is the hydrogen ion activity coefficient and x_{H^+} is the aqueous mole fraction of
3 dissociated H^+ . The presence of aerosol water is implicit in this definition since free H^+ cannot
4 exist in solid particles. Second, ‘aerosol acidity’ is commonly used to describe the loading of
5 protons in atmospheric particles, in units of nmol m^{-3} or neq m^{-3} . This definition can take several
6 forms, including aerosol strong acidity (H^+ contributed by strong acids that dissociate completely
7 at most pH), free acidity (dissociated H^+), or total acidity (includes free H^+ and the undissociated
8 H^+ bound to weak acids), typically defined by the measurement approach (Keene et al., 2004;
9 Lawrence and Koutrakis, 1996). The major difference between aerosol pH and the proton
10 loading is that pH is the H^+ concentration per liquid water volume (i.e., aerosol water) while the
11 aerosol proton loading is the H^+ concentration per unit volume of air. Aerosol pH is the
12 parameter of interest for the atmospheric phenomena described above, but the proton loading is
13 often treated as a surrogate for pH. This is a critical distinction that will be discussed in detail
14 below, especially in relation to the appropriate use of each parameter for the analysis of chemical
15 processes in the atmosphere.

16 **2.1 Ion Balance Method**

17 The ion balance method is commonly employed to estimate the proton loading in
18 atmospheric particles. This method is based upon the principle of electroneutrality, and assumes
19 that any deficit in measured cationic charge compared to measured anionic charge is due to the
20 presence of protons, according to:

21 $[H^+] = \sum n_i[anion_i] - \sum n_i[cation_i]$ (2)

1 where n_i is the charge of species i , and $[anion_i]$ and $[cation_i]$ are the molar concentrations of
2 anion and cation species, respectively. If the sum of measured cations exceeds that of the
3 measured anions, then the difference is attributed to OH^- . H^+ levels under an anion deficit are
4 then calculated from the inferred $[\text{OH}^-]$ using the water dissociation constant, K_w . Most
5 applications of the ion balance use inorganic ions only, even though organic acids can be
6 important to the interpretation of aerosol acidity in diverse locations (Lawrence and Koutrakis,
7 1996; Metzger et al., 2006; Trebs et al., 2005), especially at relatively low acidities where
8 organic acids dissociate and contribute to the ion balance. Neglecting this effect will lead to
9 biases in the inferred H^+ . Organic compounds can also form salt complexes with inorganic
10 species (e.g., ammonium oxalate) (Reid et al., 1998; Paciga et al., 2014), further indicating the
11 importance of organic acids in the ion balance.

12 **2.2 Molar Ratio**

13 While the ion balance method is used to estimate the absolute proton loading in
14 atmospheric particles, the molar ratio is independent of absolute concentrations. The molar ratio
15 is a ratio of the total molar concentration of measured inorganic cations to the measured
16 inorganic anions:

$$17 \text{ Molar ratio} = \frac{\Sigma(\text{cations})}{\Sigma(\text{anions})} \quad (3)$$

18 It is also frequently employed as an equivalence (charge) ratio. The concept was first introduced
19 in thermodynamic models to define major ions and composition domains (e.g., Pilinis and
20 Seinfeld, 1987; Nenes et al., 1998; Kim et al., 1993; Fountoukis and Nenes, 2007), but never to
21 infer the levels of acidity and pH. Thermodynamic models using the major species/composition
22 domain approach (e.g., Fountoukis and Nenes, 2007) consider the possibility that aerosol species
23 may volatilize enough to affect the ratio at equilibrium. Furthermore, the degree of dissociation

1 of species such as $\text{H}_2\text{SO}_4/\text{HSO}_4^-/\text{SO}_4^{2-}$, $\text{HNO}_3/\text{NO}_3^-$, HCl/Cl^- , and $\text{NH}_3/\text{NH}_4^+$ can affect the value
2 of the ratio. In subsequent studies; however, the molar ratio has been treated as a proxy for
3 acidity, with lower ratios corresponding to particles with the highest levels of acidity (lowest pH)
4 (e.g., Kerminen et al., 2001). Molar ratios that yield a charge balance (i.e., equivalence ratios of
5 unity or greater) are assumed for fully neutralized aerosol. Two common simplifications of the
6 molar ratio approach are often applied when the concentrations of crustal elements are relatively
7 low (e.g., Zhang et al., 2007):

$$8 \quad \text{Molar ratio} = \text{NH}_4^+ / (\text{Cl}^- + \text{NO}_3^- + 2 * \text{SO}_4^{2-}) \quad (4)$$

9 and (e.g., Peltier et al., 2007; Tanner et al., 2009; Froyd et al., 2010):

$$10 \quad \text{Molar ratio} = \text{NH}_4^+ / (2 * \text{SO}_4^{2-}) \quad (5)$$

11 **2.3 Thermodynamic Equilibrium Models**

12 Multiple thermodynamic equilibrium models have been developed to predict the behavior
13 – most commonly the phase partitioning, liquid water content, and chemical speciation – of
14 inorganic aerosol precursors. Previous studies have performed detailed comparisons and have
15 explored the causes of disagreement among different thermodynamic equilibrium models (Ansari
16 and Pandis, 1999; Zhang et al., 2000). We do not attempt to repeat this exercise. Instead,
17 thermodynamic models are considered as one method to estimate the acidity of atmospheric
18 particles. Two models are used in the present analysis: ISORROPIA-II (Fountoukis and Nenes,
19 2007; Nenes et al., 1999) and the Extended Aerosol Inorganics Model (E-AIM) (Clegg et al.,
20 1998; Clegg et al., 2003; Wexler and Clegg, 2002). ISORROPIA-II was designed with high
21 computational efficiency to facilitate its incorporation in large-scale models and has seen wide
22 usage. E-AIM is computationally expensive but is considered the benchmark since it employs
23 few assumptions in its calculation of aerosol inorganic behavior (Zaveri et al., 2008).

1 Two applications of each model are considered (Fountoukis et al., 2009): (a) “forward”
 2 (or “closed”) mode calculations, in which inputs to the model include T, RH and the total (gas +
 3 aerosol) concentrations of aerosol precursors in the air parcel, and, (b) “reverse” (or “open”)
 4 calculations, in which inputs to the model include T, RH and the concentration of aerosol
 5 species. The output of both calculations is the concentration of species in the gas and aerosol
 6 (solid/liquid) phases, pH, and aerosol water. Highly time-resolved measurements of aerosol
 7 composition (e.g., via PILS-IC or AMS) are frequently conducted without the corresponding
 8 gas-phase aerosol precursor measurements (HCl, HNO₃, NH₃). Under this condition, it is
 9 conceptually straightforward to run the thermodynamic models in “reverse” mode, and this
 10 approach is frequently applied to analyze ambient and experimental data. In this analysis, we
 11 consider aerosol acidity predictions using both methods.

12 **2.4 Phase Partitioning**

13 Aerosol pH can also be estimated from the phase partitioning of certain semi-volatile
 14 compounds, such as HNO₃/NO₃⁻, NH₃/NH₄⁺, and HCl/Cl⁻ (e.g., Keene et al., 2004; Meskhidze et
 15 al., 2003). The H⁺ concentration in aqueous particles can be calculated assuming that the system
 16 is in equilibrium (using NH₃/NH₄⁺ as an example):



19 Under this approach, both the gas-phase and aerosol ionic components are measured, and the
 20 liquid H⁺ concentration can be calculated after combining the equilibrium expressions from
 21 reactions 1 and 2:

$$22 \{H^+\} = \frac{K_w\{NH_4^+\}}{K_H K_b p_{NH_3}} \quad (6)$$

1 where $\{H^+\}$ is the activity of H^+ in atmospheric particles, K_H is the temperature-dependent
2 Henry's law constant, K_b is the temperature-dependent base dissociation constant, K_w is the
3 temperature-dependent water dissociation constant, p_{NH_3} is the gas-phase partial pressure of
4 ammonia, and $\{NH_4^+\}$ is the activity of aqueous aerosol ammonium. The aerosol liquid water
5 content is required to derive $\{NH_4^+\}$ (e.g., to convert from $\mu\text{g m}^{-3}$ to mol L^{-1}). The H^+ and NH_4^+
6 activity coefficients can also be calculated from thermodynamic equilibrium models in order to
7 convert concentrations to activities, although the simplifying assumption of $\gamma = 1$ is sometimes
8 employed, with satisfactory results (Fountoukis and Nenes, 2007).

9 **2.5 Evaluation Dataset**

10 We evaluate the above methods using ground-based data collected during the MILAGRO
11 campaign at the T1 site in Mexico City (Molina et al., 2010). The measurements spanned 10
12 March - 1 April 2006 (Table 1). Inorganic $PM_{2.5}$ composition (Na^+ , NH_4^+ , K^+ , Mg^{2+} , Ca^{2+} , Cl^- ,
13 NO_3^- , and SO_4^{2-}) was measured with a Particle-into-Liquid Sampler coupled to a dual ion
14 chromatograph (Hennigan et al., 2008). Six-minute integrated measurements were conducted
15 every 15 min. Given that $PM_{2.5}$ composition only was measured, no size-acidity dependence
16 could be elucidated (Keene et al., 2002). Ammonia was measured with a quantum cascade laser
17 spectrometer with 1-min sample time resolution (Aerodyne Research, Inc.). Nitric acid was
18 measured with 5-min time resolution via thermal dissociation-laser induced fluorescence of
19 nitrogen oxides (Day et al., 2002; Farmer et al., 2011). All chloride was assumed to reside in the
20 particle phase (i.e., gas-phase HCl was effectively zero), which was determined to be a valid
21 assumption given the high concentration of gas-phase NH_3 (Fountoukis et al., 2009).

22 The chemical measurements, along with ambient temperature and RH, were used as
23 inputs into ISORROPIA-II and E-AIM. Fountoukis et al. (2009) evaluated the equilibrium

1 partitioning of semi-volatile compounds at T1 using ISORROPIA-II. We do not duplicate that
2 effort here: instead, we focus solely on particle acidity and the comparison across the different
3 proxy methods described above. For the ‘reverse’ model runs, the 1-min met data were averaged
4 on the aerosol sampling times and were used in conjunction with the aerosol concentrations as
5 model inputs. Given the differences in sample timing, the ‘forward’ model runs used as inputs
6 the total gas + aerosol concentrations and met data averaged onto common 10-min sample times.
7 Output from the reverse model runs was used for the present analysis only if the following
8 criteria were met for a given sample: 1) NH_4^+ , NO_3^- , and SO_4^{2-} aerosol measurements were
9 operational, 2) $\text{RH} > 40\%$, and 3) modeled aerosol liquid water > 0 . Output from the forward
10 model runs was used for the present analysis only if the above criteria were met, and both the
11 NH_3 and HNO_3 measurements were operational for a given sampling interval. These constraints
12 explain the differences in sample numbers between the forward and reverse simulations and
13 between E-AIM and ISORROPIA (Table 2). ISORROPIA-II model runs were performed in
14 ‘metastable’ mode where the aerosol is only in the aqueous phase and can be supersaturated
15 (<http://isorropia.eas.gatech.edu/>). ISORROPIA treats the Na^+ - NH_4^+ - K^+ - Ca^{2+} - Mg^{2+} - Cl^- - NO_3^- -
16 SO_4^{2-} system. For conditions of excess cations, ISORROPIA-II assumes that bicarbonate
17 (HCO_3^-) and carbonate (CO_3^{2-}) account for the deficit and a pH limit of 7 is imposed. Model
18 version AIM-IV was used for RH conditions greater than 60% ($n = 348$, Table 2) and model
19 version AIM-II was used for RH conditions between 40-60% ($n = 112$, Table 2)
20 (<http://www.aim.env.uea.ac.uk/aim/aim.php>). AIM-IV treats the Na^+ - NH_4^+ - Cl^- - NO_3^- - SO_4^{2-}
21 system while AIM-II treats NH_4^+ - NO_3^- - SO_4^{2-} . For AIM, measured cations not treated by the
22 model were accounted for as equivalent sodium (Na^*) in AIM-IV and equivalent ammonium
23 (NH_4^*) in AIM-II. Cl^- was accounted for as equivalent sulfate (SO_4^*) in AIM-II. Ion balance is

1 required for all simulations in E-AIM: any cation deficit was balanced using H^+ while any anion
2 deficit was balanced using OH^- since these are also required model inputs. E-AIM assumes that
3 OH^- balances any excess cations, rather than carbonate, and thus has regions of higher predicted
4 aerosol pH compared with ISORROPIA.

5 E-AIM model runs were performed in solid + liquid mode where salts precipitate once
6 the aqueous solution becomes saturated. Overall, strong similarities between E-AIM and
7 ISORROPIA suggest that the choice of metastable vs. stable (solid + liquid) mode did not
8 appreciably affect the predicted aerosol pH levels. Given the importance of aerosol liquid water,
9 data below 40% RH were excluded from the analysis. During the MILAGRO study, this was
10 approximately 50% of the total measurement period. Further, points above 40% RH with
11 modeled aerosol liquid water content of zero were excluded from the analysis since a pH cannot
12 be derived for these samples. This was the cause of differences in sample numbers between the
13 E-AIM and ISORROPIA simulations (Table 2).

14 **3 Results and Discussion**

15 **3.1 Thermodynamic Equilibrium Models**

16 Thermodynamic equilibrium models are frequently used to estimate aerosol acidity. Prior
17 studies have observed and discussed large differences in aerosol acidity predicted by different
18 models (Ansari and Pandis, 1999; Yao et al., 2006); we do not revisit this analysis, but instead
19 seek to understand some of the limitations and uncertainties of using thermodynamic equilibrium
20 models to predict aerosol pH. Figure 1 shows that a large source of uncertainty is tied to the
21 availability of gas-phase data and whether the model is run in the forward (gas + aerosol inputs)
22 or reverse (aerosol inputs only) mode. Note that the number of forward mode predictions was

1 less than the reverse mode predictions due to availability of coincident aerosol and gas-phase
 2 measurements. For ISORROPIA and E-AIM, the median differences between the models run in
 3 forward and reverse modes were 3.5 and 3.1 pH units, respectively. This finding is consistent
 4 with a modeling study of aerosol pH in Hong Kong, as well (Yao et al., 2006). Other
 5 parameters, such as aerosol liquid water, have much closer agreement between the forward and
 6 reverse modes (not shown), given that it is largely driven by total aerosol mass and thus, is much
 7 less sensitive to gas-phase species.

8 The large differences in the forward-reverse mode predictions of aerosol pH seen in Fig.
 9 1 come about for several reasons. Upon specification of the aerosol species and surrounding RH
 10 and T, thermodynamic models first determine the aerosol pH and liquid water content (assuming
 11 that a liquid phase can exist), followed by computing the concentration of gas-phase semi-
 12 volatile compounds in equilibrium with the aerosol (e.g., NH₃, HNO₃ and HCl). The aerosol pH
 13 is largely driven by electroneutrality in the aqueous phase, as any imbalance between charges
 14 from cations and anions needs to be balanced by H⁺ and OH⁻:

$$15 \quad [H^+] + \sum_{n^+}[X^+] = [OH^-] + \sum_{n^-}[Y^-], \text{ or } [H^+] + I_b - [OH^-] = 0 \quad (7)$$

16 where $I_b = \sum_{n^+}[X^+] - \sum_{n^-}[Y^-]$, is the ion balance parameter, n^+ and n^- are the number of
 17 positively and negatively charged ionic species, respectively, and $[X^+]$ is the concentration of a
 18 species in the aqueous phase, in gram equivalents (geq). In the case where the aerosol is acidic
 19 (i.e., pH < 7 or $I_b < -\sqrt[2]{K_w}$, with $K_w = [OH^-][H^+]$) then $[OH^-]$ contributes negligibly to I_b ,
 20 and $[H^+] \cong -I_b$. Similarly, when the aerosol is alkaline (i.e., pH > 7 or $I_b > \sqrt[2]{K_w}$) then $[H^+]$
 21 contributes negligibly to I_b , $[OH^-] \cong I_b$ and $[H^+] = K_w/[OH^-]$.

1 Given the above, one can construct a diagram that relates aerosol pH to I_b ; this is shown in Fig.
2 2. It is noteworthy that pH changes considerably over a narrow range of I_b , when the value of I_b
3 is close to zero. For acidic and very alkaline aerosol, uncertainty in I_b – shown as the (a) and (c)
4 regions of Fig. 2 – may introduce a 0.5-1.0 pH unit bias in predicted pH. In region (b) however,
5 a small uncertainty in I_b leads to shifts in pH that spans effectively 10 pH units (or more). This
6 uncertainty may come from either uncertainty in the measurements, themselves, or from
7 approximations such as the exclusion of minor species (e.g., crustal elements) from the analysis.
8 The data used in Fig. 2 are hypothetical – values of I_b ranging from -1 to 1 at a constant aerosol
9 loading were input under conditions of constant T and RH to generate the predicted pH.
10 However, Fig. 3 shows that for the MILAGRO dataset, the predicted aerosol pH (reverse mode)
11 is extremely sensitive to minor uncertainties in the measurement inputs, and thus, to uncertainties
12 in I_b . Fig. 3 shows the sensitivity in predicted aerosol pH under the reverse mode calculation to
13 +/-10% changes in the aerosol NH_4^+ concentration. The aerosol pH differed by more than 1.0
14 pH units for 18% of the data when NH_4^+ increased by 10%. Likewise, aerosol pH differed by
15 more than 1.0 pH units for 12% of the data when NH_4^+ decreased by 10%. Similar sensitivities
16 were also observed for +/- 10% changes in aerosol NO_3^- and SO_4^{2-} inputs. Using gas + aerosol
17 inputs strongly constrains the effects of measurement errors and therefore is thought to give a
18 more accurate representation of aerosol partitioning and composition (Fountoukis et al., 2009;
19 Guo et al., 2014). Our results support this thought, and indicate that reverse mode calculations of
20 aerosol H^+ and pH should likely be avoided for the interpretation of experimental data. The
21 exception to this recommendation would be a system that contains very low concentrations of
22 semi-volatiles. Without accompanying gas-phase data to constrain the thermodynamic models,
23 an alternate approach that may yield a more accurate representation of aerosol pH is the use of

1 aerosol concentrations as input in forward mode calculations. In the southeastern US, Guo et al.
2 (2014) report that this approach led to biases in aerosol pH of ~1 pH unit, which is considerably
3 lower than the bias observed in Fig. 1, if we assume that the forward mode predictions are
4 accurate (see more discussion on this point below).

5 **3.2 Phase Partitioning**

6 Figure 4 shows aerosol pH predicted by ammonia phase partitioning vs. aerosol pH predicted by
7 E-AIM and ISORROPIA run in the forward and reverse modes. To predict aerosol pH from the
8 $\text{NH}_3/\text{NH}_4^+$ phase equilibrium (Eq. 6), aerosol liquid water was taken from the forward model
9 output of ISORROPIA. The temperature-dependent K_H and K_b are from Chameides (1984),
10 while the temperature-dependent K_w is from Stumm and Morgan (1996). We have used liquid
11 concentrations, not activities in the application of Equation 6 (i.e., activity coefficients for H^+
12 and NH_4^+ are assumed to be unity), following the approach of Keene et al. (2004). The
13 implications of these assumptions are discussed below. The best agreement between the phase
14 partitioning approach and the models was found for both forward model applications (Figs. 4a
15 and c). A slope of 0.98 and high R^2 value (0.80) indicate excellent agreement between E-AIM
16 and the phase partitioning approach (Fig. 4a). The median difference between these methods
17 was only 0.4 pH units. Likewise, good agreement was observed between ISORROPIA-II in the
18 forward mode and the phase partitioning pH (Fig. 4c, slope = 0.98 and $R^2 = 0.47$).

19 Differences between the $\text{NH}_3/\text{NH}_4^+$ phase partitioning predictions and either
20 thermodynamic model are possibly due to differences in equilibrium constants and/or differences
21 in the activity coefficients, although the former is more likely. That is evident from the strong
22 agreement seen in Fig. 4a; since E-AIM employs activity coefficient calculations for all species,
23 our calculation using concentrations instead of activities does not appear to systematically bias

1 the phase partitioning pH predictions. A detailed characterization of uncertainties and
2 sensitivities of the various methods to differences in equilibrium constants and activity
3 coefficients is beyond the scope of this study, but should be explored in the future.

4 The above results were contrasted by very poor agreement between the reverse models
5 and phase partitioning predictions of aerosol pH (Figs. 4b and d). The median difference
6 between aerosol pH predicted by NH₃ phase partitioning and E-AIM run in the reverse mode was
7 3.5 pH units (n = 72). Similarly, the median difference between aerosol pH predicted by NH₃
8 phase partitioning and ISORROPIA-II run in reverse mode was 3.1 pH units (n = 72). These
9 large differences are consistent with the large differences observed between the forward and
10 reverse predictions of pH (Fig. 1). These results are also consistent with large discrepancies (of
11 order 1-4 pH units) in aerosol pH between E-AIM run in the reverse mode and the phase
12 partitioning approach for a study in Hong Kong (Yao et al., 2006). As discussed above, gas +
13 aerosol inputs constrain the effects of measurement uncertainty on thermodynamic models, and
14 thus, the large differences observed in Fig. 4b and d provide further support that the reverse
15 model applications are challenged to accurately predict aerosol pH. For the MILAGRO data set,
16 approximately half of all reverse model runs predicted pH values less than 0 (44% for E-AIM,
17 51% for ISORROPIA). This is inconsistent with the observed aerosol ammonium fraction (NH₄⁺
18 / (NH₃ + NH₄⁺)), which was only 0.2, on average, over the study period. Under conditions
19 typical of the MILAGRO study (293 K, 10 μg m⁻³ aerosol liquid water, total NH₃ of 10-30 μg m⁻³),
20 if the aerosol pH is less than 0, thermodynamic calculations predict that essentially all of the
21 NH₃ will partition to the particle phase at equilibrium. The fact that gas-phase NH₃ was
22 abundant (Table 1) suggests either: 1) the system is not at equilibrium, or 2) aerosol pH > 0.
23 Fountoukis et al. (2009) found that the equilibration timescales for NH₃/NH₄⁺ (approximately 10

1 min) were on par with the measurement integration timescales during MILAGRO, strongly
2 suggesting that the assumption of equilibrium is valid. This further supports the conclusion
3 above that the reverse mode models vastly overstate the acidity (underestimate pH) of the
4 Mexico City aerosol.

5 These results suggest that the two best proxy methods for estimating aerosol pH are: 1)
6 thermodynamic equilibrium models run using gas + aerosol inputs, and 2) the phase partitioning
7 of ammonia. Under certain conditions, the phase partitioning of $\text{HNO}_3/\text{NO}_3^-$ gives similar results
8 to that of ammonia (Young et al., 2013), so this is another feasible approach. It should be noted
9 that Young et al. (2013) caution against the use of HCl/Cl^- partitioning to estimate pH on the
10 basis of large (order of magnitude) uncertainty in the Henry's law constant for HCl. It should
11 also be noted that Keene et al. (2004) observed relatively poor agreement between pH predicted
12 by ammonia and nitric acid phase partitioning. This may be due to the explicit treatment of
13 activity coefficients (as was done by Young et al. (2013)), or to differences in other factors such
14 as relative ammonia levels, since this can introduce major differences in thermodynamic model
15 predictions (Ansari and Pandis, 1999). Other limitations of the phase partitioning approach
16 should be considered, depending on the environment. This includes long equilibration
17 timescales for coarse particles, and the presence of insoluble or partially soluble salts (Jacobson,
18 1999; Fridlind and Jacobson, 2000; Meng and Seinfeld, 1996).

19 **3.3 Ion Balance vs. Aerosol pH**

20 Figure 5a shows a probability distribution for the ion balance during MILAGRO. All of the
21 measured inorganic species (Section 2.5) were included in the calculation according to Equation
22 2 but dissociated organic acids were not included since they were not measured. Approximately
23 75% of the paired cation-anion measurements had a cation deficit and would thus be inferred as

1 acidic according to the ion balance. Figure 5b shows the aerosol pH predicted by E-AIM
2 (reverse mode) vs. the inorganic ion balance. The data follow the traditional titration curve
3 shape, with those points having a negative ion balance (anions > cations) all having predicted pH
4 below 3.0 and points having a positive ion balance (cations > anions) all having predicted pH
5 above 7.8.

6 The ion balance proxy method assumes that conditions of high aerosol H^+ loading (in
7 $nmol\ m^{-3}$) correspond to an aerosol distribution with a low (acidic) pH (e.g., Guo et al., 2012;
8 Feng et al., 2012; Zhang et al., 2012a). Figure 6 shows the relationship between predicted
9 aerosol pH and the H^+ concentration inferred from the ion balance. An anion deficit in the ion
10 balance is assumed to be due to OH^- (Equation 2) - implying extremely low H^+ levels - so only
11 data with a negative ion balance were included in this analysis ($n = 340$). Figure 6 shows no
12 correlation at all between the H^+ loading and the predicted aerosol pH using either the forward
13 (Fig. 6a) or reverse models (Fig. 6b). Note the differences in pH predicted by the forward and
14 reverse models, as observed in Fig. 1. Numerous points in the lowest H^+ quartile have pH levels
15 below the median pH of the upper H^+ quartile (Fig. 6b). Similarly, for a given H^+ loading, a
16 wide pH range of ~2-3 pH units is typically predicted. This wide pH range is observed across all
17 H^+ loadings, even at the high and low ends, because aerosol liquid water content and the H^+
18 activity coefficient can differ dramatically for a given H^+ level. The ion balance method is
19 insensitive to either of these factors that are critical in determining aerosol pH (equation 1).
20 Pathak et al. (2009) found a similar disconnect between H^+ inferred from the ion balance and
21 predicted aerosol pH for measurements in four cities across China.

22 A further problem with the ion balance is that it is unable to distinguish between free and
23 undissociated H^+ (e.g., protons associated with bisulfate (HSO_4^-)) (Keene et al., 2004). This

1 limitation becomes very important when the solution pH approaches the pK_a of any major ion
2 that is associated with acidity, including HNO_3 , HCl , and NH_3 . The pK_a of HSO_4^- is 1.99
3 (Stumm and Morgan, 1996), and at pH levels below 3, the bisulfate/sulfate equilibrium begins to
4 shift appreciably towards the protonated form, implying that the ion balance overestimates H^+ .
5 This is illustrated in Fig. 7a and 7b, which show the H^+ levels inferred from the ion balance
6 compared to the H^+ loadings predicted by E-AIM and ISORROPIA (both run in reverse mode),
7 respectively. Although the thermodynamic models use electroneutrality to derive H^+ , they
8 account for partial dissociation, which explains why the ion balance gives H^+ levels that are ~45-
9 65% higher than the models. The discrepancy in pH predicted by the forward and reverse mode
10 thermodynamic calculations (Fig. 1 and Fig. 6) also implies large differences in the predicted
11 aerosol H^+ loadings. Figure 7c and d shows H^+ levels inferred from the ion balance compared to
12 H^+ levels predicted by E-AIM and ISORROPIA, both run in forward mode. The forward mode
13 thermodynamic calculations predict H^+ levels that are orders of magnitude lower than either the
14 ion balance or reverse mode calculations, consistent with the large differences in predicted pH
15 shown in Fig. 1. This is also consistent with large discrepancies in H^+ levels in Pittsburgh, PA
16 predicted by forward (Takahama et al., 2006) and reverse (Zhang et al., 2007) thermodynamic
17 equilibrium model simulations. Although the measurement periods for these studies did not
18 overlap, the similar NH_4^+ and SO_4^{2-} concentrations suggest that the large differences in aerosol
19 H^+ were likely due to differences in the forward and reverse model simulations, not in the actual
20 pH levels of the aerosol.

21 Finally, another major limitation in estimating the aerosol H^+ loading from the ion
22 balance is high uncertainty in H^+ that comes about from the propagation of measurement error.
23 Figure 8a shows the relative ion balance uncertainty (%) vs. the ion balance loading ($nmol\ m^{-3}$).

1 Note that the points with a negative ion balance (orange trace in Fig. 8a) are inferred as the H⁺
2 loading, and so this trace also represents the uncertainty in H⁺ from the ion balance. The ion
3 balance uncertainty was calculated using a standard propagation of error technique (Harris,
4 1999):

$$5 \quad u_{IB} = (u_{Na^+}^2 + u_{NH_4^+}^2 + u_{Mg^{2+}}^2 + u_{Ca^{2+}}^2 + u_{K^+}^2 + u_{Cl^-}^2 + u_{NO_3^-}^2 + u_{SO_4^{2-}}^2)^{1/2} \quad (8)$$

6 where u_{IB} is the absolute uncertainty in the ion balance (in neq m⁻³), and the terms on the right
7 hand side represent the absolute uncertainties in each inorganic species in neq m⁻³ (Na⁺, NH₄⁺,
8 Mg²⁺, Ca²⁺, K⁺, Cl⁻, NO₃⁻, and SO₄²⁻), calculated assuming 10% relative uncertainty for each
9 species. Figure 8a shows that the relative ion balance (and [H⁺]) uncertainty ($u_{IB}/[\text{ion balance}]$)
10 grows with decreasing ion balance (or [H⁺]), as one would expect. A frequency distribution of
11 the ion balance uncertainty from the MILAGRO study shows that approximately 40% of the ion
12 balance (and [H⁺]) calculations had an associated uncertainty higher than 50%, and more than
13 20% of the ion balance (and [H⁺]) calculations had an associated uncertainty higher than 100%
14 (Fig. 8b).

15 These results demonstrate numerous problems with the ion balance and strongly suggest
16 that it is inadequate to represent the pH of atmospheric particles. The ion balance may provide a
17 qualitative indication of acidic conditions when anions far exceed cations, but the variable effects
18 of liquid water, the buffering action of HSO₄⁻/SO₄²⁻, and the effect of species activity coefficients
19 in concentrated particles precludes its use for any quantitative means. Even when all ionic
20 components – including the dissociated ions of organic acids – are accounted for and measured
21 with good precision, the ion balance is unlikely to qualitatively distinguish alkaline particles
22 from mildly acidic particles due to the propagation of uncertainties in the aerosol composition
23 measurements. This recommendation against the use of the ion balance as a proxy for aerosol

1 pH is supported by prior work (Keene and Savoie, 1998; Winkler, 1986; Guo et al., 2014). The
2 H^+ concentration derived from the ion balance is often just a surrogate for sulfate, especially in
3 environments where sulfate is the dominant inorganic species (Pathak et al., 2009; Zhang et al.,
4 2007). It is possible – likely even – to simultaneously have particles with a low concentration of
5 H^+ (in $nmol\ m^{-3}$) that are highly acidic (low pH). Studies that infer the effects of particle acidity
6 on atmospheric chemical processes using the inorganic ion balance are likely flawed. For
7 example, correlations between SOA and aerosol H^+ concentrations (from the ion balance) have
8 been interpreted as evidence for acid-catalyzed SOA formation (Feng et al., 2012; Guo et al.,
9 2012; Budisulistiorini et al., 2013; Pathak et al., 2011; Nguyen et al., 2014; Zhang et al., 2012a).
10 These studies may have misinterpreted their data, since sulfate may actually be a limiting factor
11 in isoprene and monoterpene SOA formation (Xu et al., 2015). H^+ derived from the ion balance
12 is a surrogate for sulfate and many factors lead to correlations between sulfate and SOA in
13 regional pollution (Sun et al., 2011; Zhang et al., 2012b).

14 **3.4 Molar Ratio vs. pH**

15 Similar to applications of the ion balance, the molar ratio is frequently used as a proxy for
16 aerosol pH. Molar ratios that yield a charge balance (i.e., equivalence ratios of unity or greater)
17 are assumed for fully neutralized aerosol while decreasing cation/anion ratios are assumed to
18 represent decreasing aerosol pH (He et al., 2012; Kerminen et al., 2001; Huang et al., 2013). The
19 data and assumptions that underlie the molar ratio method are the same as those used to calculate
20 the ion balance. Thus, many of the same limitations apply to the molar ratio method. The
21 exclusion of minor ionic species, including crustal elements and dissociated organic acids, can
22 significantly bias the results (Cao et al., 2013; Jacobson, 1999; Trebs et al., 2005; Ziemba et al.,
23 2007; Moya et al., 2002). The propagation of analytical uncertainty can also create problems

1 with the signal-to-noise ratio for many samples that will challenge the interpretations of the
2 molar ratio. Finally, the molar ratio does not account for the effects of aerosol water or species
3 activities on particle acidity. Given the similar assumptions and limitations, it should be
4 unsurprising that $[H^+]$ from the ion balance was highly correlated with the cation/anion molar
5 ratio ($R^2 = 0.66$, not shown) for the MILAGRO dataset. Similar to the ion balance results, no
6 correlation was observed between the molar ratio and forward-mode predicted aerosol pH (Fig.
7 9). Zhang et al. (2007) and Behera et al. (2014) demonstrated similar problems translating the
8 molar ratio into aerosol pH for studies in Pittsburgh and Singapore, respectively. Even under the
9 limiting case when 1) crustal elements were low (where NH_4^+ , Cl^- , NO_3^- , and SO_4^{2-} together
10 accounted for greater than 95% of inorganic aerosol ion mass) and 2) the aerosol regime was
11 inferred to be highly acidic (samples with $NH_4^+/(Cl^- + NO_3^- + 2*SO_4^{2-})$ molar ratios less than
12 0.75), there was no correlation between the molar ratio and predicted pH (Fig. 10).

13 These results indicate that the molar ratio is not a suitable proxy to infer the acidity of
14 atmospheric particles. This applies to all variations of the molar ratio (Equations 3, 4, or 5).
15 When the majority of inorganic species (> 95%) are accounted for, the molar ratio is able to
16 distinguish alkaline particles from acidic particles with good reliability; however, it is unable to
17 provide any measure – even qualitative – of the degree of aerosol acidity. The lack of
18 relationship between the molar ratio and predicted aerosol pH strongly suggests problems with
19 studies that have used the molar ratio as a proxy for pH. For example, studies that have
20 attempted to characterize the occurrence of acid-catalyzed SOA formation in the atmosphere
21 may have incorrectly interpreted the aerosol acidity using a molar ratio approach (e.g., Tanner et
22 al., 2009; Peltier et al., 2007; Zhang et al., 2007; Froyd et al., 2010).

1 **4 Conclusions**

2 We have carried out an analysis of proxy methods used to estimate the pH of atmospheric
3 particles. The ion balance method, which is used to infer the aerosol H^+ loading, showed no
4 correlation with aerosol pH predicted by multiple independent metrics. This indicates that
5 conditions of increasing H^+ loading do not necessarily correspond to decreasing (i.e., more
6 acidic) aerosol pH. Likewise, the cation/anion molar ratio (and related metrics) showed no
7 relationship with different predictions of aerosol pH. When species accounting for greater than
8 95% of inorganic aerosol mass were included in the analysis, the molar ratio appears to reliably
9 distinguish acidic from alkaline particles; however, the molar ratio should not be treated as a
10 surrogate for aerosol pH. The molar ratio actually showed a strong relationship with the ion
11 balance. A major reason for the inability of these methods to represent aerosol pH is that both
12 neglect the effects of aerosol water and partial dissolution of ions and acids on pH, in accordance
13 with previously published studies (Keene and Savoie, 1998; Winkler, 1986). Further, the ion
14 balance and molar ratio can also be severely limited by signal-to-noise ratio due to analytical
15 uncertainties. These results strongly discourage the use of the ion balance or molar ratio for pH
16 or H^+ inference.

17 These results also suggest that thermodynamic equilibrium models require both gas +
18 aerosol inputs for accurate predictions of H^+ and pH. Two independent models - E-AIM and
19 ISORROPIA - performed similarly and predict much lower pH (more acidic particles) in the
20 reverse modes using aerosol inputs only. The aerosol pH levels predicted by both reverse
21 models do not agree with either the pH predictions using gas + aerosol inputs or the phase
22 partitioning of ammonia. The models in reverse mode predict highly acidic particles for
23 extended periods of time (i.e., $pH < 0$), despite high concentrations of gas-phase ammonia and

1 relatively short equilibration timescales. Further, the models in reverse mode are highly
2 sensitive to uncertainty in the measurement inputs: small deviations in major aerosol species on
3 the order of common aerosol measurement uncertainties can induce changes in predicted pH that
4 exceed 10 pH units. This recommendation is consistent with other studies that show much better
5 model performance when aerosol + gas inputs are used (Fountoukis et al., 2009; Guo et al.,
6 2014).

7 Thermodynamic equilibrium models in forward mode had very good agreement with pH
8 predicted by the phase partitioning of ammonia. These methods are largely, but not completely
9 independent, as the aerosol liquid water required for the phase partitioning calculation is
10 obtained from the same thermodynamic models. In addition, the use of activity coefficients from
11 thermodynamic models as inputs in the phase partitioning calculations would further couple the
12 two methods (here we have avoided this by using concentrations instead of activities).

13 Thermodynamic equilibrium models are generally quite skilled in predicting aerosol liquid water
14 (Khlystov et al., 2005), so this likely introduces minimal uncertainty to the present analysis. In
15 regions where organics are high, their contribution to aerosol liquid water (and hence, pH)
16 should be investigated (Guo et al., 2014). The fact that these largely independent methods
17 agreed so closely provides the basis for the recommendation of their use to estimate the pH of
18 atmospheric particles. As with the application of thermodynamic equilibrium models, the phase
19 partitioning approach makes the implicit assumption that the gas/particle system is at
20 equilibrium. This appears to be a good assumption for the Mexico City data set (Fountoukis et
21 al., 2009), but it can be a poor assumption when coarse particles are abundant, such as in the
22 marine environment (Fridlind and Jacobson, 2000). The phase partitioning approach is also
23 likely limited in ammonia-poor environments where all or most of the ammonia resides in the

1 aerosol phase. In such environments, the phase partitioning of nitric acid may be a good
2 alternative if both nitric acid and aerosol nitrate concentrations are high enough (Young et al.,
3 2013; Meskhidze et al., 2003). Uncertainty in the Henry's law constant of other compounds,
4 especially HCl, may limit the application of the phase partitioning approach beyond $\text{NH}_3/\text{NH}_4^+$
5 and $\text{HNO}_3/\text{NO}_3^-$ (Young et al., 2013).

6 Our recommendation for the use of the phase partitioning approach and forward
7 equilibrium model calculations to best predict aerosol pH contradicts the recommendations in a
8 similar study (Yao et al., 2006). Both our study (from Mexico City) and the Yao et al. (2006)
9 study (Hong Kong) agree that E-AIM run in the reverse mode yields predicted aerosol pH levels
10 significantly lower than the phase partitioning or forward model predictions. We differ on our
11 interpretation of the results: Yao et al. (2006) conclude that the phase partitioning approach and
12 forward model calculations erroneously assume that the gas-aerosol system has reached
13 equilibrium, even though their analysis is based upon 12- and 24-h $\text{PM}_{2.5}$ measurements. This
14 sampling time should far-exceed the equilibration time for sub-micron particles, which is on the
15 order of seconds-to-minutes (Meng and Seinfeld, 1996). In addition, our comparisons in Fig. 4a
16 and 4c only include the subset of data where RH exceeds 60%, a region in which the
17 thermodynamic predictions – and assumption of equilibrium – become more accurate (Moya et
18 al., 2002). Fountoukis et al. (2009) examined the equilibrium assumption for $\text{PM}_{2.5}$ during
19 MILAGRO and found it to be valid. Thus, we believe that the forward thermodynamic models
20 and phase partitioning approach are far more accurate in their predictions of pH than the reverse
21 models run in closed mode without the additional constraint of gas-phase data.

22 These recommendations should be evaluated in other environments with different
23 chemical characteristics and meteorology than was observed during MILAGRO. In particular,

1 the recommendations should be evaluated in ammonia poor environments, since thermodynamic
2 equilibrium models often diverge in their predictions under such conditions (Ansari and Pandis,
3 1999). Despite their uncertainties, thermodynamic models and phase partitioning provide the
4 best methods to estimate the pH of fine atmospheric particles. Other widely used metrics – ion
5 balance and ion ratios – are misleading and should be avoided beyond the establishment of
6 general alkalinity or acidity. Hence, conclusions that are sensitive to aerosol pH but that are
7 based upon the ion balance or molar ratio may need revision.

8 **Acknowledgements**

9 The authors gratefully acknowledge the use of NH₃ data from M. L. Fischer (Environmental
10 Energy Technologies Division, Lawrence Berkeley National Laboratory), and HNO₃ data from
11 R. C. Cohen (Department of Chemistry, University of California, Berkeley) and D. K. Farmer
12 (Department of Chemistry, Colorado State University). We also gratefully acknowledge useful
13 conversations with J. G. Murphy (Department of Chemistry, University of Toronto).

14

1 **Tables**

2 **Table 1:** Overview of MILAGRO measurements used as modeling inputs

3

4 **Measurement Overview**

Species	Measurement dates (2006)	Study n	Mean		
			Concentration \pm 1σ ($\mu\text{g m}^{-3}$)	5 th percentile ($\mu\text{g m}^{-3}$)	95 th percentile ($\mu\text{g m}^{-3}$)
Na ⁺	10 Mar – 1 Apr	998	0.31 \pm 0.14	0.18	0.45
NH ₄ ⁺	10 Mar – 1 Apr	1159	1.69 \pm 1.36	0.25	4.43
Ca ²⁺	10 Mar – 1 Apr	1654	0.53 \pm 0.57	0.02 ^a	1.64
Mg ²⁺	10 Mar – 1 Apr	1051	0.15 \pm 0.07	0.08	0.28
Cl ⁻	10 Mar – 1 Apr	1603	0.27 \pm 0.69	0.02 ^a	1.23
NO ₃ ⁻	10 Mar – 1 Apr	1634	2.93 \pm 2.66	0.37	8.20
SO ₄ ²⁻	10 Mar – 1 Apr	1652	3.74 \pm 2.30	1.63	8.05
*NH ₃	21 Mar – 31 Mar	9594	25.2 \pm 15.3	7.9	56.1
*HNO ₃	17 Mar – 30 Mar	430	2.43 \pm 1.48	0.71	5.11

5 *concentrations in ppb

6 ^aThis value represents the measurement LOD

7

8 **Table 2:** Overview of modeling outputs and criteria

9

10 **Modeling Overview**

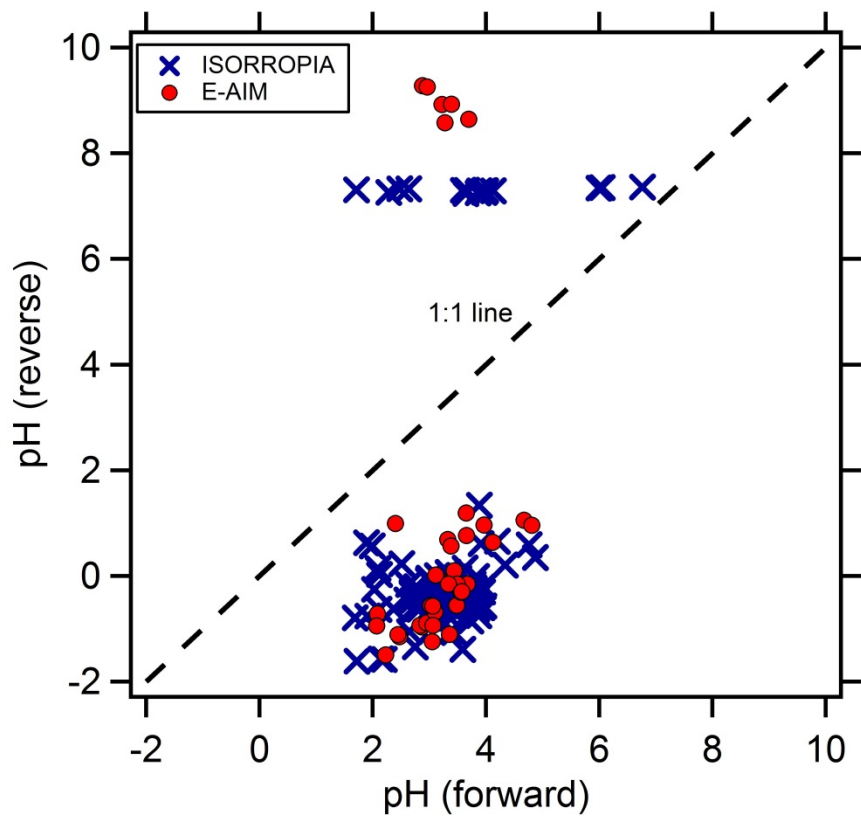
Model	n	Average [H ⁺] (nmol m ⁻³)	Median [H ⁺] (nmol m ⁻³)	Average pH	Median pH
ISORROPIA-II, Reverse ¹	438	19.39	10.34	1.98	-0.02
E-AIM, Reverse ¹	460	15.77	6.56	2.36	0.14
ISORROPIA-II, Forward ²	89	0.008	0.005	3.31	3.38
E-AIM, Forward ²	39	0.015	0.012	3.24	3.32

11 ¹Output limited to samples meeting these criteria: 1) NH₄⁺, NO₃⁻, and SO₄²⁻ > 0; 2) RH \geq 40%;
 12 and 3) modeled aerosol liquid water content > 0.

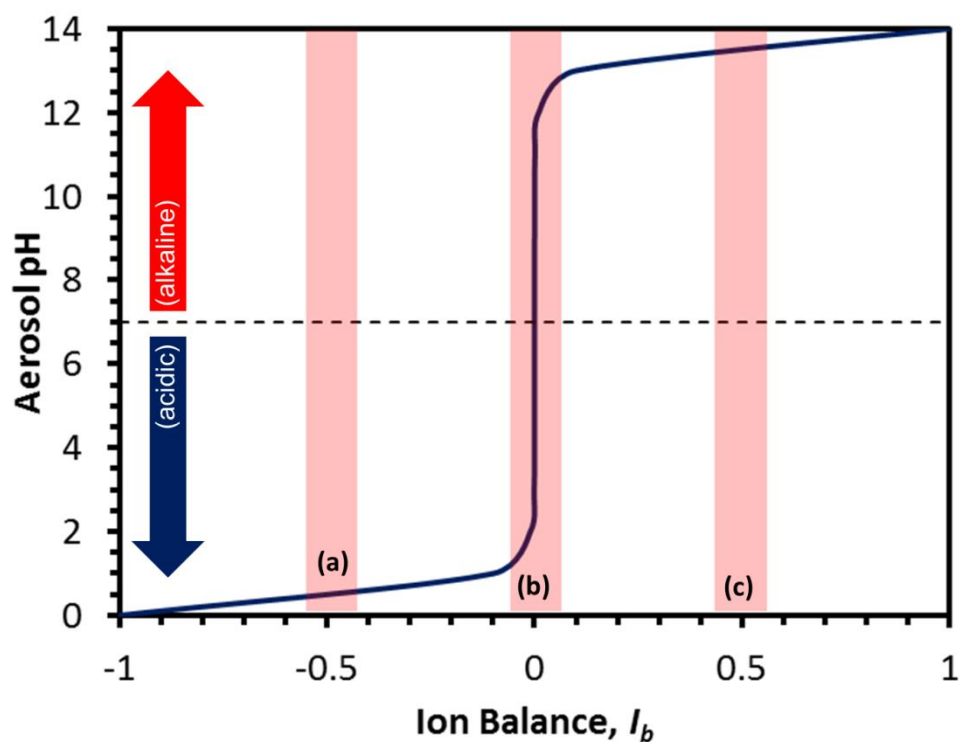
13 ²Output limited to samples meeting these criteria: 1) NH₄⁺, NO₃⁻, SO₄²⁻, NH₃, and HNO₃ > 0; 2)
 14 RH \geq 40%; and 3) modeled aerosol liquid water content > 0.

15

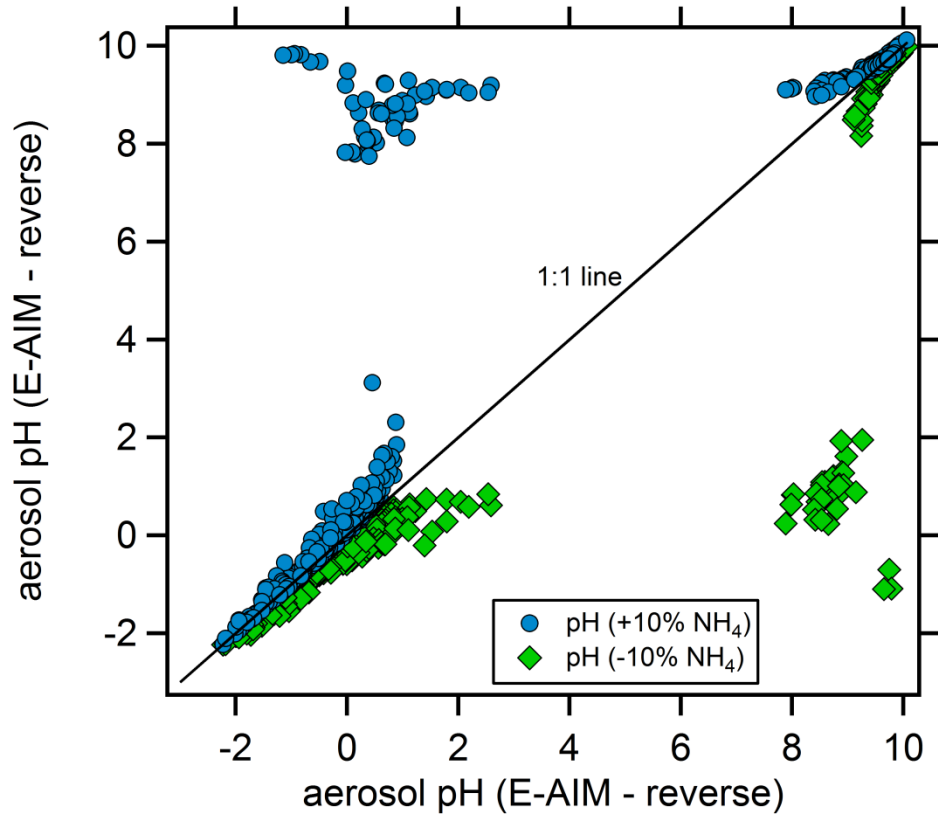
16



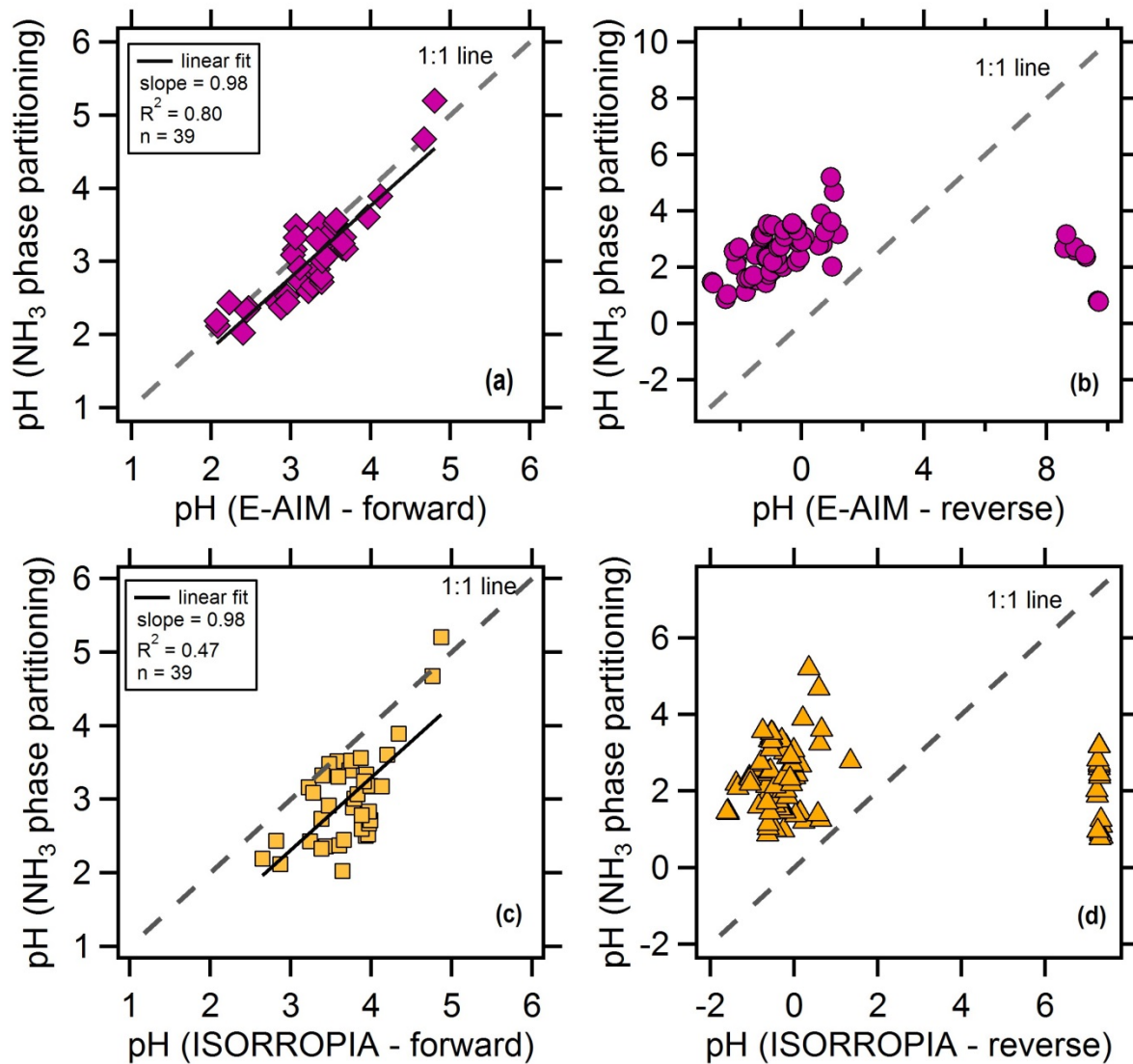
1
2 Fig. 1. Comparison of pH predicted using the reverse and forward modes of ISORROPIA and E-
3 AIM.



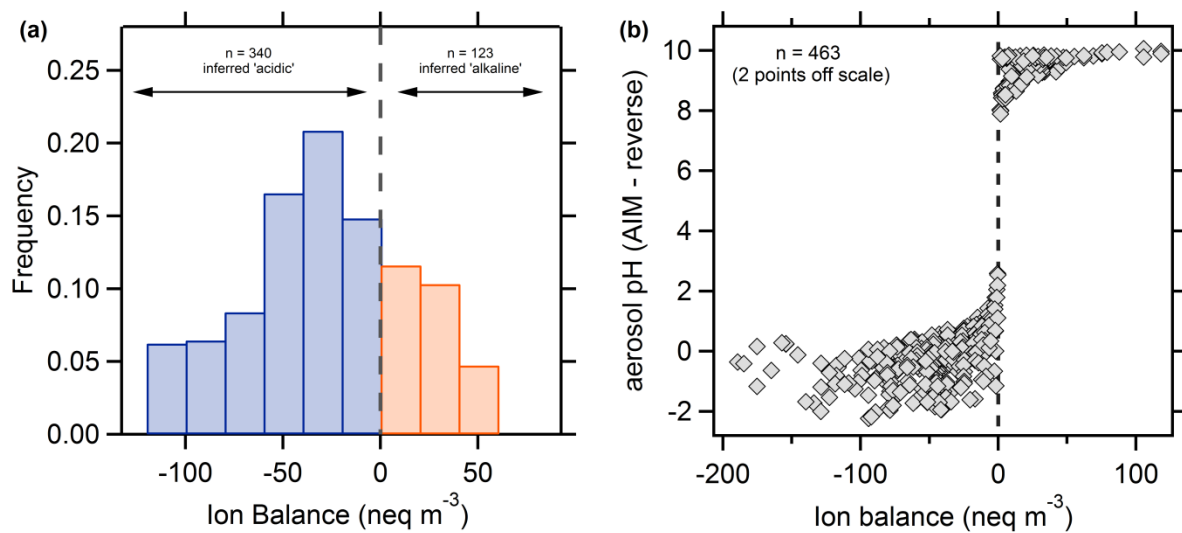
1
 2 Fig. 2. Aerosol pH as a function of the parameter I_b (see Eq. 7 for explanation). The data used
 3 here are hypothetical – values of I_b ranging from -1 to 1 at a constant aerosol loading were input
 4 under conditions of constant T and RH to demonstrate the extreme sensitivity of aerosol pH at I_b
 5 values near 0.0 (region ‘b’).



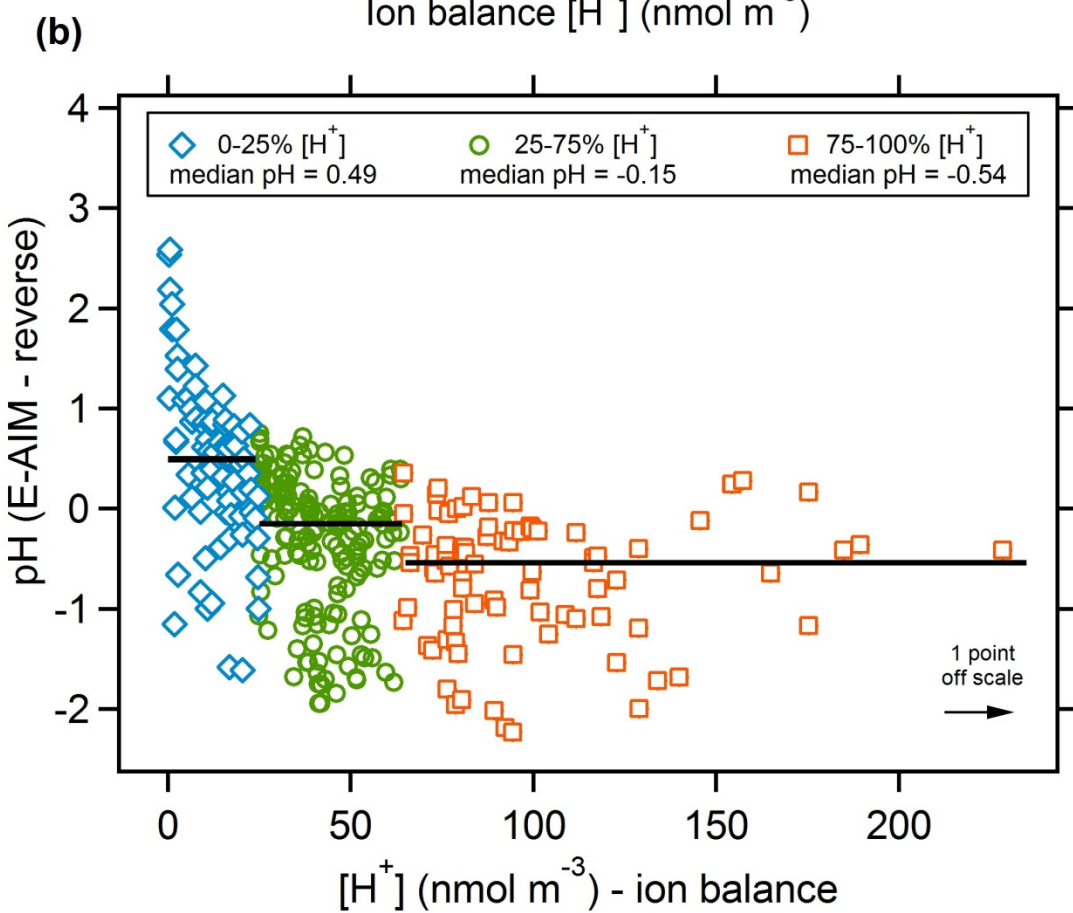
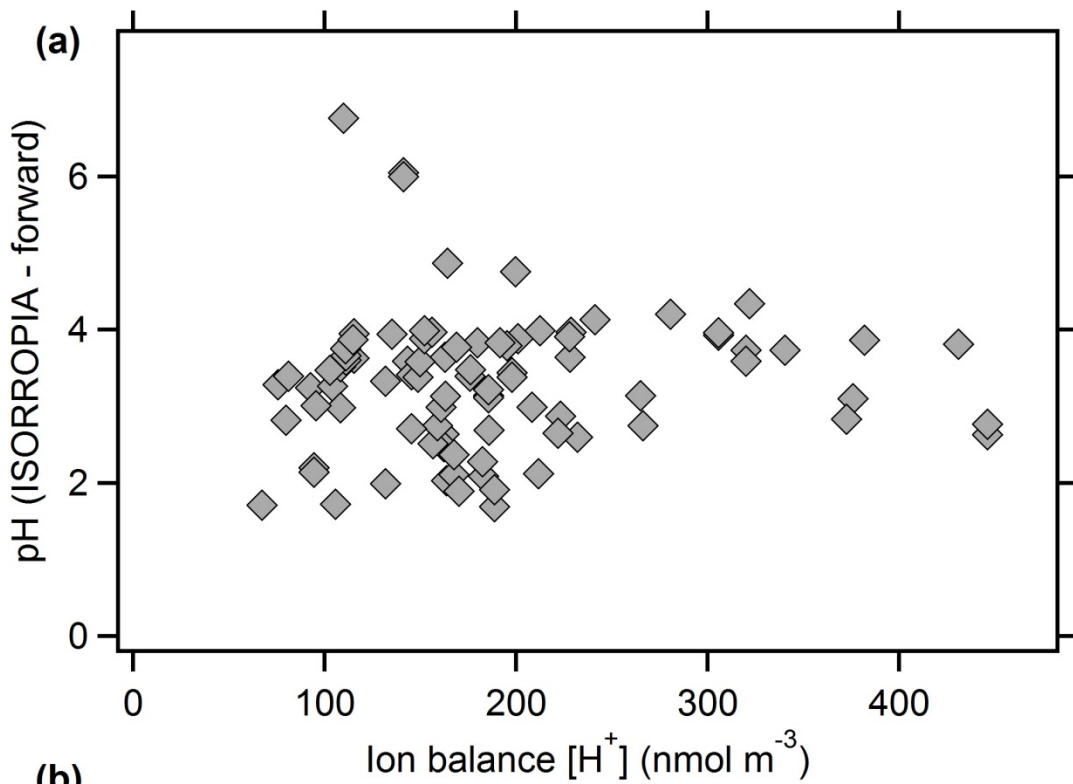
1
2 Fig. 3. Sensitivity of aerosol pH predicted with E-AIM (reverse mode) to small changes in the
3 input aerosol NH_4^+ concentration.



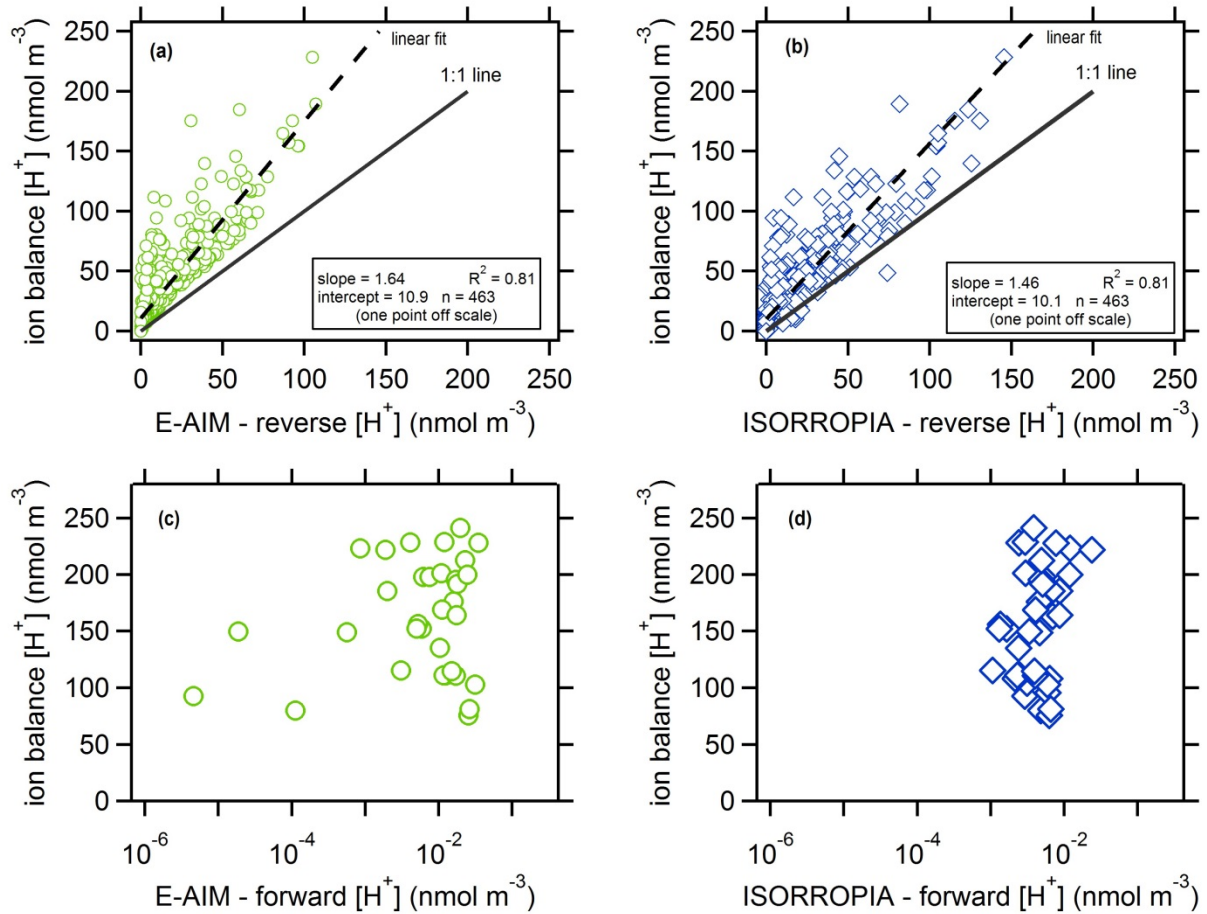
1
 2 Fig. 4. Aerosol pH predicted by the phase partitioning of ammonia compared to pH predicted by
 3 (a) E-AIM in the forward mode, (b) E-AIM in the reverse mode, (c) ISORROPIA in the forward
 4 mode, and (d) ISORROPIA in the reverse mode.



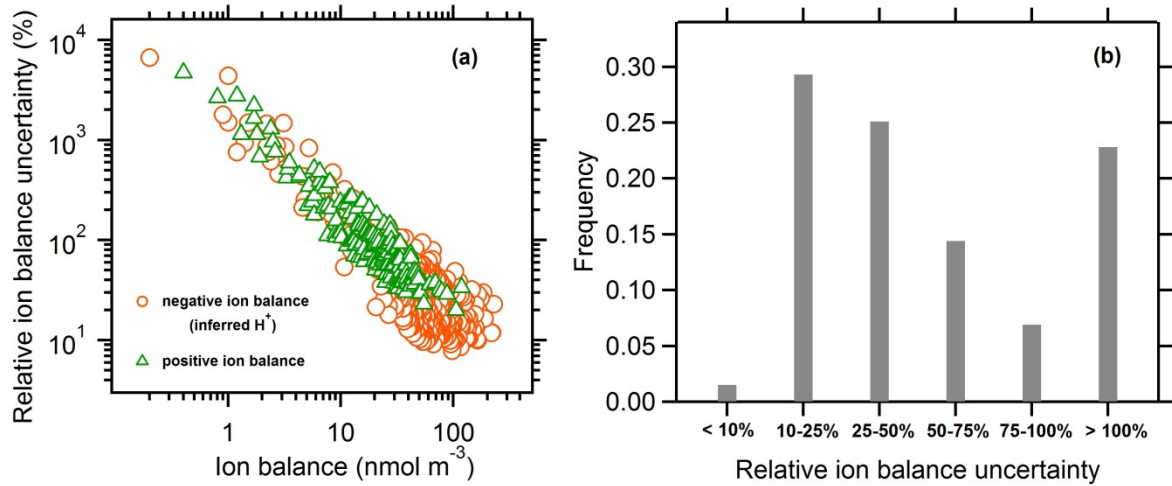
1
 2 Fig. 5. (a) Frequency distribution of the aerosol ion balance during MILAGRO, and (b) aerosol
 3 pH predicted by E-AIM in the reverse mode vs. the ion balance. The dashed lines at 0 serve as a
 4 visual reference for neutral particles.



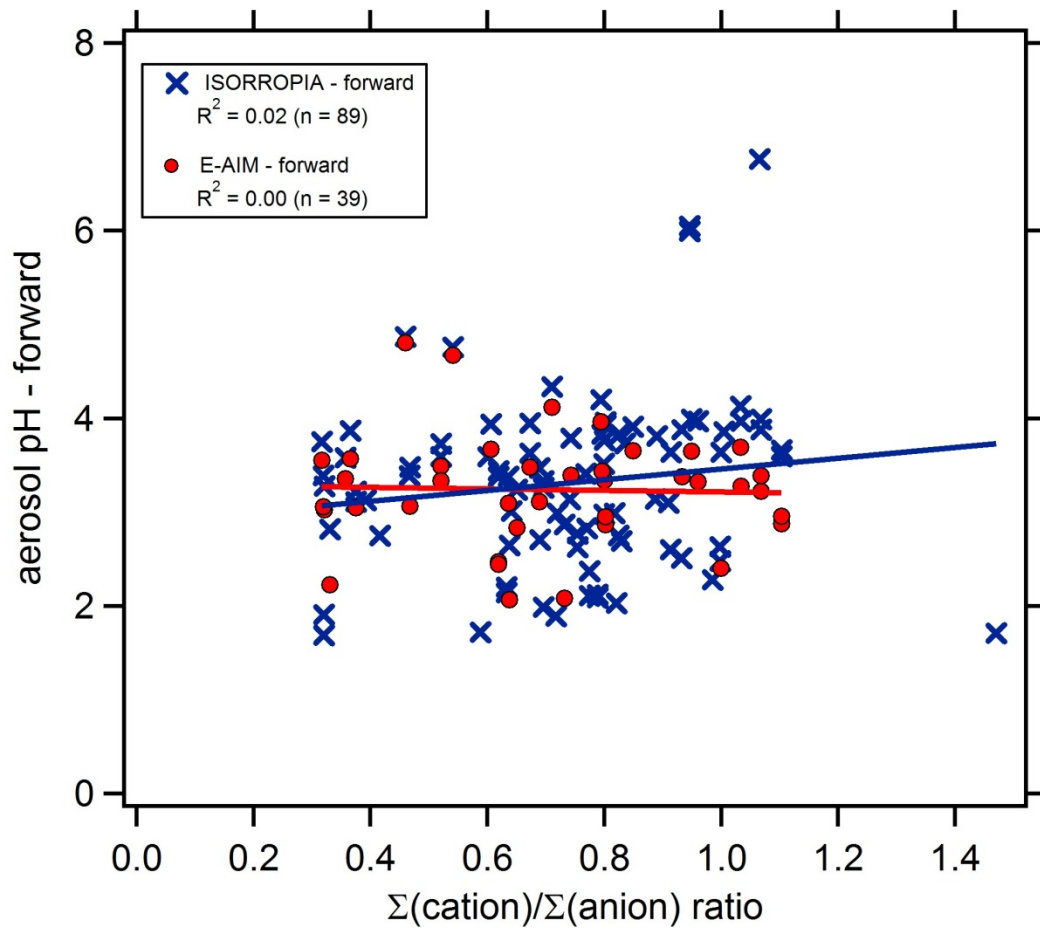
1 Fig. 6. (a) aerosol pH predicted by ISORROPIA in the forward mode vs. the H^+ concentration
 2 derived from the ion balance, and (b) aerosol pH predicted by E-AIM in the reverse mode vs. the
 3 H^+ concentration derived from the ion balance. Only points with a cation charge deficit
 4 ($\Sigma(\text{anions}) > \Sigma(\text{cations})$) are included in the analysis. The horizontal black bars represent the
 5 medians corresponding to the values in the legend.



6
 7 Fig. 7. H^+ levels inferred from the ion balance compared to H^+ levels predicted by (a) E-AIM in
 8 the reverse mode, (b) ISORROPIA in the reverse mode, (c) E-AIM in the forward mode, and (d)
 9 ISORROPIA in the forward mode. Note the log scale for the x-axes in (c) and (d).



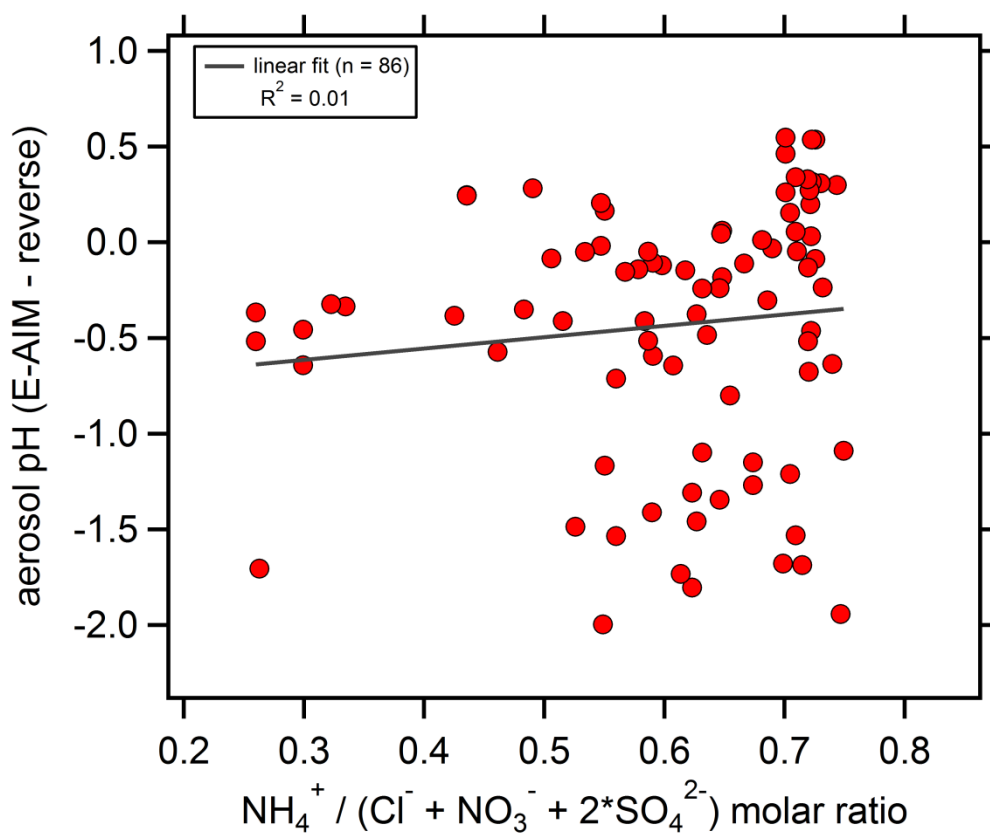
1
 2 Fig. 8. (a) Relative ion balance uncertainty (%) as a function of the ion balance level. Note that
 3 the orange trace represents [H⁺], and so this trace also represents the uncertainty in [H⁺] from the
 4 ion balance. (b) Frequency distribution in the relative ion balance uncertainty.
 5



1

2 Fig. 9. Aerosol pH predicted by the forward mode equilibrium models compared to the

3 $\Sigma(\text{cations})/\Sigma(\text{anions})$ charge ratio.



1
 2 Fig. 10. Predicted aerosol pH vs. the $\text{NH}_4^+ / (\text{Cl}^- + \text{NO}_3^- + 2 \cdot \text{SO}_4^{2-})$ molar ratio, using only data
 3 where the ratio is less than 0.75 (region inferred as highly acidic) and where $\Sigma(\text{NH}_4^+ + \text{Cl}^- +$
 4 $\text{NO}_3^- + \text{SO}_4^{2-})$ accounts for greater than 95% of measured inorganic aerosol mass (i.e., with low
 5 crustal concentrations).

6

7

1 **References**

- 2 Ahrens, L., Harner, T., Shoeib, M., Lane, D. A., and Murphy, J. G.: Improved Characterization
3 of Gas-Particle Partitioning for Per- and Polyfluoroalkyl Substances in the Atmosphere
4 Using Annular Diffusion Denuder Samplers, *Environ Sci Technol*, 46, 7199-7206, Doi
5 10.1021/Es300898s, 2012.
- 6 Ansari, A. S., and Pandis, S. N.: An analysis of four models predicting the partitioning of
7 semivolatile inorganic aerosol components, *Aerosol Sci Tech*, 31, 129-153, Doi
8 10.1080/027868299304200, 1999.
- 9 Behera, S., Cheng, J., and Balasubramanian, R.: In situ acidity and pH of size-fractionated
10 aerosols during a recent smoke-haze episode in Southeast Asia, *Environ Geochem*
11 *Health*, 1-17, 10.1007/s10653-014-9660-1, 2014.
- 12 Brown, S. S., Thornton, J. A., Keene, W. C., Pszenny, A. A. P., Sive, B. C., Dube, W. P.,
13 Wagner, N. L., Young, C. J., Riedel, T. P., Roberts, J. M., VandenBoer, T. C., Bahreini,
14 R., Ozturk, F., Middlebrook, A. M., Kim, S., Hubler, G., and Wolfe, D. E.: Nitrogen,
15 Aerosol Composition, and Halogens on a Tall Tower (NACHTT): Overview of a
16 wintertime air chemistry field study in the front range urban corridor of Colorado, *J*
17 *Geophys Res-Atmos*, 118, 8067-8085, Doi 10.1002/Jgrd.50537, 2013.
- 18 Budisulistiorini, S. H., Canagaratna, M. R., Croteau, P. L., Marth, W. J., Baumann, K., Edgerton,
19 E. S., Shaw, S. L., Knipping, E. M., Worsnop, D. R., Jayne, J. T., Gold, A., and Surratt, J.
20 D.: Real-Time Continuous Characterization of Secondary Organic Aerosol Derived from
21 Isoprene Epoxydiols in Downtown Atlanta, Georgia, Using the Aerodyne Aerosol
22 Chemical Speciation Monitor, *Environ Sci Technol*, 47, 5686-5694, Doi
23 10.1021/Es400023n, 2013.
- 24 Cao, J. J., Tie, X. X., Dabberdt, W. F., Jie, T., Zhao, Z. Z., An, Z. S., Shen, Z. X., and Feng, Y.
25 C.: On the potential high acid deposition in northeastern China, *J Geophys Res-Atmos*,
26 118, 4834-4846, Doi 10.1002/Jgrd.50381, 2013.
- 27 Chameides, W. L.: The photochemistry of a remote marine stratiform cloud, *Journal of*
28 *Geophysical Research: Atmospheres*, 89, 4739-4755, 10.1029/JD089iD03p04739, 1984.
- 29 Clegg, S. L., Brimblecombe, P., and Wexler, A. S.: Thermodynamic model of the system H^+ -
30 NH_4^+ - SO_4^{2-} - NO_3^- - H_2O at tropospheric temperatures, *J Phys Chem A*, 102, 2137-2154,
31 Doi 10.1021/Jp973042r, 1998.
- 32 Clegg, S. L., Seinfeld, J. H., and Edney, E. O.: Thermodynamic modelling of aqueous aerosols
33 containing electrolytes and dissolved organic compounds. II. An extended Zdanovskii-
34 Stokes-Robinson approach, *J Aerosol Sci*, 34, 667-690, DOI 10.1016/s0021-
35 8502(03)00019-3, 2003.
- 36 Day, D. A., Wooldridge, P. J., Dillon, M. B., Thornton, J. A., and Cohen, R. C.: A thermal
37 dissociation laser-induced fluorescence instrument for in situ detection of NO_2 , peroxy
38 nitrates, alkyl nitrates, and HNO_3 , *J Geophys Res-Atmos*, 107, Artn 4046Doi
39 10.1029/2001jd000779, 2002.
- 40 Dockery, D. W., Cunningham, J., Damokosh, A. I., Neas, L. M., Spengler, J. D., Koutrakis, P.,
41 Ware, J. H., Raizenne, M., and Speizer, F. E.: Health effects of acid aerosols on North
42 American children: Respiratory symptoms, *Environ Health Persp*, 104, 500-505, Doi
43 10.2307/3432990, 1996.

1 Farmer, D. K., Perring, A. E., Wooldridge, P. J., Blake, D. R., Baker, A., Meinardi, S., Huey, L.
2 G., Tanner, D., Vargas, O., and Cohen, R. C.: Impact of organic nitrates on urban ozone
3 production, *Atmos Chem Phys*, 11, 4085-4094, DOI 10.5194/acp-11-4085-2011, 2011.

4 Feng, J. L., Guo, Z. G., Zhang, T. R., Yao, X. H., Chan, C. K., and Fang, M.: Source and
5 formation of secondary particulate matter in PM_{2.5} in Asian continental outflow, *J*
6 *Geophys Res-Atmos*, 117, Artn D03302Doi 10.1029/2011jd016400, 2012.

7 Fountoukis, C., and Nenes, A.: ISORROPIA II: a computationally efficient thermodynamic
8 equilibrium model for K^+ - Ca^{2+} - Mg^{2+} - NH_4^+ - Na^+ - SO_4^{2-} - NO_3^- - Cl^- - H_2O aerosols, *Atmos*
9 *Chem Phys*, 7, 4639-4659, 2007.

10 Fountoukis, C., Nenes, A., Sullivan, A., Weber, R., Van Reken, T., Fischer, M., Matias, E.,
11 Moya, M., Farmer, D., and Cohen, R. C.: Thermodynamic characterization of Mexico
12 City aerosol during MILAGRO 2006, *Atmos Chem Phys*, 9, 2141-2156, 2009.

13 Fridlind, A. M., and Jacobson, M. Z.: A study of gas-aerosol equilibrium and aerosol pH in the
14 remote marine boundary layer during the First Aerosol Characterization Experiment
15 (ACE 1), *J Geophys Res-Atmos*, 105, 17325-17340, Doi 10.1029/2000jd900209, 2000.

16 Froyd, K. D., Murphy, S. M., Murphy, D. M., de Gouw, J. A., Eddingsaas, N. C., and Wennberg,
17 P. O.: Contribution of isoprene-derived organosulfates to free tropospheric aerosol mass,
18 *P Natl Acad Sci USA*, 107, 21360-21365, DOI 10.1073/pnas.1012561107, 2010.

19 Gaston, C. J., Riedel, T. P., Zhang, Z., Gold, A., Surratt, J. D., and Thornton, J. A.: Reactive
20 Uptake of an Isoprene-derived Epoxydiol to Submicron Aerosol Particles, *Environ Sci*
21 *Technol*, 10.1021/es5034266, 2014.

22 Guo, H., Xu, L., Bougiatioti, A., Cerully, K., Capps, S. L., Hite, J. R., Carlton, A. G., Lee, S.-H.,
23 Bergin, M. H., Ng, N. L., Nenes, A., and Weber, R. J.: Particle water and pH in the
24 southeastern United States, *Atmos. Chem. Phys. Discuss.*, 14, 27143-27193,
25 doi:10.5194/acpd-14-27143-2014, 2014.

26 Guo, S., Hu, M., Guo, Q. F., Zhang, X., Zheng, M., Zheng, J., Chang, C. C., Schauer, J. J., and
27 Zhang, R. Y.: Primary Sources and Secondary Formation of Organic Aerosols in Beijing,
28 China, *Environ Sci Technol*, 46, 9846-9853, Doi 10.1021/Es20425641, 2012.

29 Gwynn, R. C., Burnett, R. T., and Thurston, G. D.: A time-series analysis of acidic particulate
30 matter and daily mortality and morbidity in the Buffalo, New York, region, *Environ*
31 *Health Persp*, 108, 125-133, Doi 10.2307/3454510, 2000.

32 Harris, D. C.: Quantitative Chemical Analysis, 5th Ed. ed., W. H. Freeman and Company, New
33 York, 1999.

34 He, K., Zhao, Q., Ma, Y., Duan, F., Yang, F., Shi, Z., and Chen, G.: Spatial and seasonal
35 variability of PM_{2.5} acidity at two Chinese megacities: insights into the formation of
36 secondary inorganic aerosols, *Atmos Chem Phys*, 12, 1377-1395, DOI 10.5194/acp-12-
37 1377-2012, 2012.

38 Hennigan, C. J., Sullivan, A. P., Fountoukis, C. I., Nenes, A., Hecobian, A., Vargas, O., Peltier,
39 R. E., Hanks, A. T. C., Huey, L. G., Lefer, B. L., Russell, A. G., and Weber, R. J.: On the
40 volatility and production mechanisms of newly formed nitrate and water soluble organic
41 aerosol in Mexico City, *Atmos Chem Phys*, 8, 3761-3768, 2008.

42 Huang, Y., Li, L., Li, J., Wang, X., Chen, H., Chen, J., Yang, X., Gross, D. S., Wang, H., Qiao,
43 L., and Chen, C.: A case study of the highly time-resolved evolution of aerosol chemical
44 and optical properties in urban Shanghai, China, *Atmos Chem Phys*, 13, 3931-3944, DOI
45 10.5194/acp-13-3931-2013, 2013.

1 Jacobson, M. Z.: Studying the effects of calcium and magnesium on size-distributed nitrate and
2 ammonium with EQUISOLV II, *Atmos Environ*, 33, 3635-3649, Doi 10.1016/S1352-
3 2310(99)00105-3, 1999.

4 Jang, M., Cao, G., and Paul, J.: Colorimetric particle acidity analysis of secondary organic
5 aerosol coating on submicron acidic aerosols, *Aerosol Sci Tech*, 42, 409-420, Doi
6 10.1080/02786820802154861, 2008.

7 Johnson, A. H., Moyer, A., Bedison, J. E., Richter, S. L., and Willig, S. A.: Seven Decades of
8 Calcium Depletion in Organic Horizons of Adirondack Forest Soils, *Soil Sci Soc Am J*,
9 72, 1824-1830, DOI 10.2136/sssaj2006.0407, 2008.

10 Keene, W. C., Sander, R., Pszenny, A. A. P., Vogt, R., Crutzen, P. J., and Galloway, J. N.:
11 Aerosol pH in the marine boundary layer: A review and model evaluation, *J Aerosol Sci*,
12 29, 339-356, Doi 10.1016/S0021-8502(97)10011-8, 1998.

13 Keene, W. C., and Savoie, D. L.: The pH of deliquesced sea-salt aerosol in polluted marine air,
14 *Geophys Res Lett*, 25, 2181-2184, Doi 10.1029/98gl01591, 1998.

15 Keene, W. C., Pszenny, A. A. P., Maben, J. R., and Sander, R.: Variation of marine aerosol
16 acidity with particle size, *Geophys Res Lett*, 29, Artn 1101 Doi 10.1029/2001gl013881,
17 2002.

18 Keene, W. C., Pszenny, A. A. P., Maben, J. R., Stevenson, E., and Wall, A.: Closure evaluation
19 of size-resolved aerosol pH in the New England coastal atmosphere during summer, *J*
20 *Geophys Res-Atmos*, 109, Artn D23307 Doi 10.1029/2004jd004801, 2004.

21 Kerminen, V. M., Hillamo, R., Teinila, K., Pakkanen, T., Allegrini, I., and Sparapani, R.: Ion
22 balances of size-resolved tropospheric aerosol samples: implications for the acidity and
23 atmospheric processing of aerosols, *Atmos Environ*, 35, 5255-5265, Doi 10.1016/S1352-
24 2310(01)00345-4, 2001.

25 Khlystov, A., Stanier, C. O., Takahama, S., and Pandis, S. N.: Water content of ambient aerosol
26 during the Pittsburgh air quality study, *J Geophys Res-Atmos*, 110, Artn D07s10 Doi
27 10.1029/2004jd004651, 2005.

28 Kim, Y. P., Seinfeld, J. H., and Saxena, P.: Atmospheric Gas Aerosol Equilibrium 1.
29 Thermodynamic Model, *Aerosol Sci Tech*, 19, 157-181, 10.1080/02786829308959628,
30 1993.

31 Koutrakis, P., Wolfson, J. M., and Spengler, J. D.: An Improved Method for Measuring Aerosol
32 Strong Acidity: Results from a Nine-month Study in St. Louis, Missouri and Kingston,
33 Tennessee, *Atmos Environ*, 22, 6, 1988.

34 Lawrence, J., and Koutrakis, P.: Measurement and speciation of gas and particulate phase
35 organic acidity in an urban environment .2. Speciation, *J Geophys Res-Atmos*, 101,
36 9171-9184, Doi 10.1029/95jd03357, 1996.

37 Likens, G. E., Driscoll, C. T., and Buso, D. C.: Long-term effects of acid rain: Response and
38 recovery of a forest ecosystem, *Science*, 272, 244-246, DOI
39 10.1126/science.272.5259.244, 1996.

40 Mahowald, N.: Aerosol Indirect Effect on Biogeochemical Cycles and Climate, *Science*, 334,
41 794-796, DOI 10.1126/science.1207374, 2011.

42 Meng, Z. Y., and Seinfeld, J. H.: Time scales to achieve atmospheric gas-aerosol equilibrium for
43 volatile species, *Atmos Environ*, 30, 2889-2900, Doi 10.1016/1352-2310(95)00493-9,
44 1996.

- 1 Meskhidze, N., Chameides, W. L., Nenes, A., and Chen, G.: Iron mobilization in mineral dust:
2 Can anthropogenic SO₂ emissions affect ocean productivity?, *Geophys Res Lett*, 30, ArtN
3 2085 Doi 10.1029/2003gl018035, 2003.
- 4 Meskhidze, N., Chameides, W. L., and Nenes, A.: Dust and pollution: A recipe for enhanced
5 ocean fertilization?, *J Geophys Res-Atmos*, 110, ArtN D03301 Doi
6 10.1029/2004jd005082, 2005.
- 7 Metzger, S., Mihalopoulos, N., and Lelieveld, J.: Importance of mineral cations and organics in
8 gas-aerosol partitioning of reactive nitrogen compounds: case study based on MINOS
9 results, *Atmos Chem Phys*, 6, 2549-2567, 2006.
- 10 Molina, L. T., Madronich, S., Gaffney, J. S., Apel, E., de Foy, B., Fast, J., Ferrare, R., Herndon,
11 S., Jimenez, J. L., Lamb, B., Osornio-Vargas, A. R., Russell, P., Schauer, J. J., Stevens,
12 P. S., Volkamer, R., and Zavala, M.: An overview of the MILAGRO 2006 Campaign:
13 Mexico City emissions and their transport and transformation, *Atmos Chem Phys*, 10,
14 8697-8760, DOI 10.5194/acp-10-8697-2010, 2010.
- 15 Moya, M., Pandis, S. N., and Jacobson, M. Z.: Is the size distribution of urban aerosols
16 determined by thermodynamic equilibrium? An application to Southern California,
17 *Atmos Environ*, 36, 2349-2365, Pii S1352-2310(01)00549-0 Doi 10.1016/S1352-
18 2310(01)00549-0, 2002.
- 19 Nenes, A., Pandis, S. N., and Pilinis, C.: ISORROPIA: A new thermodynamic equilibrium model
20 for multiphase multicomponent inorganic aerosols, *Aquat. Geochem.*, 4, 123-152,
21 10.1023/a:1009604003981, 1998.
- 22 Nenes, A., Pandis, S. N., and Pilinis, C.: Continued development and testing of a new
23 thermodynamic aerosol module for urban and regional air quality models, *Atmos*
24 *Environ*, 33, 1553-1560, Doi 10.1016/S1352-2310(98)00352-5, 1999.
- 25 Nenes, A., Krom, M. D., Mihalopoulos, N., Van Cappellen, P., Shi, Z., Bougiatioti, A., Zarmas,
26 P., and Herut, B.: Atmospheric acidification of mineral aerosols: a source of bioavailable
27 phosphorus for the oceans, *Atmos Chem Phys*, 11, 6265-6272, DOI 10.5194/acp-11-
28 6265-2011, 2011.
- 29 Nguyen, Q. T., Christensen, M. K., Cozzi, F., Zare, A., Hansen, A. M. K., Kristensen, K.,
30 Tulinius, T. E., Madsen, H. H., Christensen, J. H., Brandt, J., Massling, A., Nojgaard, J.
31 K., and Glasius, M.: Understanding the anthropogenic influence on formation of biogenic
32 secondary organic aerosols in Denmark via analysis of organosulfates and related
33 oxidation products, *Atmos Chem Phys*, 14, 8961-8981, DOI 10.5194/acp-14-8961-2014,
34 2014.
- 35 Paciga, A. L., Riipinen, I., and Pandis, S. N.: Effect of Ammonia on the Volatility of Organic
36 Diacids, *Environ Sci Technol*, 48, 13769-13775, 10.1021/es5037805, 2014.
- 37 Pan, Y. P., Wang, Y. S., Tang, G. Q., and Wu, D.: Spatial distribution and temporal variations of
38 atmospheric sulfur deposition in Northern China: insights into the potential acidification
39 risks, *Atmos Chem Phys*, 13, 1675-1688, DOI 10.5194/acp-13-1675-2013, 2013.
- 40 Pathak, R. K., Yao, X. H., and Chan, C. K.: Sampling artifacts of acidity and ionic species in
41 PM_{2.5}, *Environ Sci Technol*, 38, 254-259, Doi 10.1021/Es0342244, 2004.
- 42 Pathak, R. K., Wu, W. S., and Wang, T.: Summertime PM_{2.5} ionic species in four major cities of
43 China: nitrate formation in an ammonia-deficient atmosphere, *Atmos Chem Phys*, 9,
44 1711-1722, 2009.
- 45 Pathak, R. K., Wang, T., Ho, K. F., and Lee, S. C.: Characteristics of summertime PM_{2.5}
46 organic and elemental carbon in four major Chinese cities: Implications of high acidity

1 for water-soluble organic carbon (WSOC), *Atmos Environ*, 45, 318-325, DOI
2 10.1016/j.atmosenv.2010.10.021, 2011.

3 Peltier, R. E., Sullivan, A. P., Weber, R. J., Wollny, A. G., Holloway, J. S., Brock, C. A., de
4 Gouw, J. A., and Atlas, E. L.: No evidence for acid-catalyzed secondary organic aerosol
5 formation in power plant plumes over metropolitan Atlanta, Georgia, *Geophys Res Lett*,
6 34, Artn L06801 Doi 10.1029/2006gl028780, 2007.

7 Pilinis, C., and Seinfeld, J. H.: Continued development of a general equilibrium model for
8 inorganic multicomponent atmospheric aerosols, *Atmos. Environ.*, 21, 2453-2466,
9 10.1016/0004-6981(87)90380-5, 1987.

10 Pszenny, A. A. P., Moldanov, J., Keene, W. C., Sander, R., Maben, J. R., Martinez, M., Crutzen,
11 P. J., Perner, D., and Prinn, R. G.: Halogen cycling and aerosol pH in the Hawaiian
12 marine boundary layer, *Atmos Chem Phys*, 4, 147-168, 2004.

13 Reid, J. S., Hobbs, P. V., Ferek, R. J., Blake, D. R., Martins, J. V., Dunlap, M. R., and Liousse,
14 C.: Physical, chemical, and optical properties of regional hazes dominated by smoke in
15 Brazil, *J Geophys Res-Atmos*, 103, 32059-32080, Doi 10.1029/98jd00458, 1998.

16 Sander, R., and Crutzen, P. J.: Model study indicating halogen activation and ozone destruction
17 in polluted air masses transported to the sea, *J Geophys Res-Atmos*, 101, 9121-9138, Doi
18 10.1029/95jd03793, 1996.

19 Schindler, D. W.: Effects of Acid-Rain on Fresh-Water Ecosystems, *Science*, 239, 149-157, DOI
20 10.1126/science.239.4836.149, 1988.

21 Stoddard, J. L., Jeffries, D. S., Lukewille, A., Clair, T. A., Dillon, P. J., Driscoll, C. T., Forsius,
22 M., Johannessen, M., Kahl, J. S., Kellogg, J. H., Kemp, A., Mannio, J., Monteith, D. T.,
23 Murdoch, P. S., Patrick, S., Rebsdorf, A., Skjelkvale, B. L., Stainton, M. P., Traaen, T.,
24 van Dam, H., Webster, K. E., Wieting, J., and Wilander, A.: Regional trends in aquatic
25 recovery from acidification in North America and Europe, *Nature*, 401, 575-578, Doi
26 10.1038/44114, 1999.

27 Stumm, W., and Morgan, J. J.: *Aquatic chemistry : chemical equilibria and rates in natural*
28 *waters*, Wiley, New York, 1996.

29 Sun, Y. L., Zhang, Q., Schwab, J. J., Demerjian, K. L., Chen, W. N., Bae, M. S., Hung, H. M.,
30 Hogrefe, O., Frank, B., Rattigan, O. V., and Lin, Y. C.: Characterization of the sources
31 and processes of organic and inorganic aerosols in New York City with a high-resolution
32 time-of-flight aerosol mass spectrometer, *Atmos Chem Phys*, 11, 1581-1602, DOI
33 10.5194/acp-11-1581-2011, 2011.

34 Surratt, J. D., Lewandowski, M., Offenberg, J. H., Jaoui, M., Kleindienst, T. E., Edney, E. O.,
35 and Seinfeld, J. H.: Effect of acidity on secondary organic aerosol formation from
36 isoprene, *Environ Sci Technol*, 41, 5363-5369, Doi 10.1021/Es0704176, 2007.

37 Takahama, S., Davidson, C. I., and Pandis, S. N.: Semicontinuous measurements of organic
38 carbon and acidity during the Pittsburgh air quality study: Implications for acid-catalyzed
39 organic aerosol formation, *Environ Sci Technol*, 40, 2191-2199, Doi
40 10.1021/Es050856+, 2006.

41 Tanner, R. L., Olszyna, K. J., Edgerton, E. S., Knipping, E., and Shaw, S. L.: Searching for
42 evidence of acid-catalyzed enhancement of secondary organic aerosol formation using
43 ambient aerosol data, *Atmos Environ*, 43, 3440-3444, DOI
44 10.1016/j.atmosenv.2009.03.045, 2009.

45 Thornton, J. A., Kercher, J. P., Riedel, T. P., Wagner, N. L., Cozic, J., Holloway, J. S., Dube, W.
46 P., Wolfe, G. M., Quinn, P. K., Middlebrook, A. M., Alexander, B., and Brown, S. S.: A

1 large atomic chlorine source inferred from mid-continental reactive nitrogen chemistry,
2 Nature, 464, 271-274, Doi 10.1038/Nature08905, 2010.

3 Trebs, I., Metzger, S., Meixner, F. X., Helas, G. N., Hoffer, A., Rudich, Y., Falkovich, A. H.,
4 Moura, M. A. L., da Silva, R. S., Artaxo, P., Slanina, J., and Andreae, M. O.: The NH_4^+ -
5 NO_3^- - Cl^- - SO_4^{2-} - H_2O aerosol system and its gas phase precursors at a pasture site in the
6 Amazon Basin: How relevant are mineral cations and soluble organic acids?, J Geophys
7 Res-Atmos, 110, Artn D07303 Doi 10.1029/2004jd005478, 2005.

8 Wexler, A. S., and Clegg, S. L.: Atmospheric aerosol models for systems including the ions H^+ ,
9 NH_4^+ , Na^+ , SO_4^{2-} , NO_3^- , Cl^- , Br^- , and H_2O , J Geophys Res-Atmos, 107, Artn 4207 Doi
10 10.1029/2001jd000451, 2002.

11 Winkler, P.: Relations Between Aerosol Acidity and Ion Balance, in: Chemistry of Multiphase
12 Atmospheric Systems, edited by: Jaeschke, W., 6, Springer-Verlag, New York, 269-298,
13 1986.

14 Xu, L., Guo, H., Boyd, C. M., Klein, M., Bougiatioti, A., Cerully, K. M., Hite, J. R., Isaacman-
15 VanWertz, G., Kreisberg, N. M., Knote, C., Olson, K., Koss, A., Goldstein, A. H.,
16 Hering, S. V., de Gouw, J., Baumann, K., Lee, S.-H., Nenes, A., Weber, R. J., and Ng, N.
17 L.: Effects of anthropogenic emissions on aerosol formation from isoprene and
18 monoterpenes in the southeastern United States, Proceedings of the National Academy of
19 Sciences, 112, 37-42, 10.1073/pnas.1417609112, 2015.

20 Yao, X. H., Ling, T. Y., Fang, M., and Chan, C. K.: Comparison of thermodynamic predictions
21 for in situ pH in PM_{2.5}, Atmos Environ, 40, 2835-2844, DOI
22 10.1016/j.atmosenv.2006.01.006, 2006.

23 Young, A. H., Keene, W. C., Pszenny, A. A. P., Sander, R., Thornton, J. A., Riedel, T. P., and
24 Maben, J. R.: Phase partitioning of soluble trace gases with size-resolved aerosols in
25 near-surface continental air over northern Colorado, USA, during winter, J Geophys Res-
26 Atmos, 118, 9414-9427, Doi 10.1002/Jgrd.50655, 2013.

27 Zaveri, R. A., Easter, R. C., Fast, J. D., and Peters, L. K.: Model for Simulating Aerosol
28 Interactions and Chemistry (MOSAIC), J Geophys Res-Atmos, 113, Artn D13204 Doi
29 10.1029/2007jd008782, 2008.

30 Zhang, H. F., Worton, D. R., Lewandowski, M., Ortega, J., Rubitschun, C. L., Park, J. H.,
31 Kristensen, K., Campuzano-Jost, P., Day, D. A., Jimenez, J. L., Jaoui, M., Offenberg, J.
32 H., Kleindienst, T. E., Gilman, J., Kuster, W. C., de Gouw, J., Park, C., Schade, G. W.,
33 Frossard, A. A., Russell, L., Kaser, L., Jud, W., Hansel, A., Cappellin, L., Karl, T.,
34 Glasius, M., Guenther, A., Goldstein, A. H., Seinfeld, J. H., Gold, A., Kamens, R. M.,
35 and Surratt, J. D.: Organosulfates as Tracers for Secondary Organic Aerosol (SOA)
36 Formation from 2-Methyl-3-Buten-2-ol (MBO) in the Atmosphere, Environ Sci Technol,
37 46, 9437-9446, Doi 10.1021/Es301648z, 2012a.

38 Zhang, Q., Jimenez, J. L., Worsnop, D. R., and Canagaratna, M.: A case study of urban particle
39 acidity and its influence on secondary organic aerosol, Environ Sci Technol, 41, 3213-
40 3219, Doi 10.1021/Es061812j, 2007.

41 Zhang, X., Liu, Z., Hecobian, A., Zheng, M., Frank, N. H., Edgerton, S., and Weber, R. J.:
42 Spatial and seasonal variations of fine particle water-soluble organic carbon (WSOC)
43 over the southeastern United States: implications for secondary organic aerosol
44 formation, Atmos Chem Phys, 12, 6593-6607, DOI 10.5194/acp-12-6593-2012, 2012b.

45 Zhang, Y., Seigneur, C., Seinfeld, J. H., Jacobson, M., Clegg, S. L., and Binkowski, F. S.: A
46 comparative review of inorganic aerosol thermodynamic equilibrium modules:

1 similarities, differences, and their likely causes, Atmos Environ, 34, 117-137, Doi
2 10.1016/S1352-2310(99)00236-8, 2000.
3 Ziemba, L. D., Fischer, E., Griffin, R. J., and Talbot, R. W.: Aerosol acidity in rural New
4 England: Temporal trends and source region analysis, J Geophys Res-Atmos, 112, Artn
5 D10s22 Doi 10.1029/2006jd007605, 2007.
6
7